

UNCLASSIFIED

AD NUMBER:

LIMITATION CHANGES

TO:

FROM:

AUTHORITY

THIS PAGE IS UNCLASSIFIED

2
DASA-1800-II



803144

DEPARTMENT OF DEFENSE
LAND FALLOUT
PREDICTION SYSTEM

Volume II
INITIAL CONDITIONS

D D C
RECEIVED
DEC 1965
RECEIVED

DASA • NDL • NRDL • TECH OPS

NOTICE

Each transmittal of this document outside the agencies of the U.S. Government must have prior approval of the Director, Defense Atomic Support Agency, Washington, D. C. 20361.

tech ops

TECHNICAL OPERATIONS RESEARCH

DASA-1800-II

DEPARTMENT OF DEFENSE LAND FALLOUT PREDICTION SYSTEM

Volume II - Initial Conditions

TO-B 66-44

30 September 1966

Prepared By

H. G. Norment, W. Y. G. Ing, and J. Zuckerman
Technical Operations Research

This research has been sponsored by the
Defense Atomic Support Agency
under NWER Subtask A7a/10.058

Submitted to

U. S. Army Nuclear Defense Laboratory
Edgewood Arsenal, Maryland

Burlington, Massachusetts

ACKNOWLEDGMENTS

The initial conditions research program, results of which are reported herein, was funded by the Defense Atomic Support Agency under Subtask A7a/10.058 through contracts DA 18-035-AMC-346(A) and DA 18-035-AMC-737(A) with the Nuclear Defense Laboratory. The authors gratefully acknowledge the contributions of Mr. R. C. Tompkins and Mr. L. M. Hardin of the Nuclear Defense Laboratory and LCDR J. W. Cane of the Defense Atomic Support Agency.

ABSTRACT

A set of initial conditions to serve as primary inputs to the Department of Defense Land Fallout Prediction System (DELFIC) is derived. The set consists of lower-boundary conditions for use by a cloud rise and growth simulation model. The conditions are time, temperature, soil burden, fraction of the soil burden in the vapor phase, and size-frequency distribution of fallout particles. The DOD Land Fallout Prediction System predicts local fallout patterns from land-surface nuclear detonations.

TABLE OF CONTENTS

	<u>Page</u>
INTRODUCTION	1
DETERMINATION OF THE INITIAL CONDITIONS	2
<u>Time of Initial Conditions Specifications</u>	3
<u>The Initial Temperature</u>	8
<u>Soil Loading of the Cloud</u>	14
<u>Background</u>	14
<u>Soil Burden Determinations for Selected Test Shots</u>	15
<u>Development of Scaling Functions</u>	18
<u>Phase Partitioning of the Soil Burden</u>	23
<u>Particle Size Frequency Distribution</u>	28
COMPUTER PROGRAM OUTLINE	30
<u>Description</u>	30
<u>Program Discussion</u>	30
<u>Operating Information</u>	31
FORTRAN LISTINGS	34
SAMPLE TEST PROBLEM AND PRINTOUT	34
REFERENCES	47
APPENDIX A. FORM OF THE TEMPERATURE EQUATION	51
REFERENCES	53
APPENDIX B. CHARACTERIZATION OF THE UNVAPORIZED PORTION OF THE CLOUD SOIL BURDEN	55
REFERENCES	64

LIST OF ILLUSTRATIONS

<u>Figure</u>	<u>Page</u>
1 Typical Cloud Dimension Plot vs. Time	4
2 Toroidal Circulation Within a Nuclear Cloud	6
3 Initial Time vs. Yield as a Function of Scaled Height of Burst	8
4 Illustrative Graph of Observed and Calculated Temperature as a Function of Time	10
5 Calculated Cloud Temperature at t_i vs. Yield as a Function of Height of Burst	13
6 Ess Isomass Contours	16
7 Intersection of a Fireball with the Ground	20
8 Calculated Total Soil Mass Lifted by the Cloud as a Function of Yield for Various Scaled Heights of Burst	22
9 Flow Chart of the Initial Conditions Module Computer Program Logic (LINK1)	30
B. 1 Illustrative Graphs That Show Relationship Between Yield and Energy Available for Heating for Several Heights of Burst	58
B. 2 Computed Temperature of Unvaporized Soil for a Surface Burst	63

INTRODUCTION

The DELFIC system calculations begin with a simulation of the nuclear cloud's rise and growth. In this simulation, a set of differential equations, which collectively describe the range of change of the system, is solved over the time interval of the cloud rise history. These differential equations are solved as an initial value problem, i.e., the integrations are done numerically for a continuous succession of small time steps that cover the time range of the cloud rise. Obviously, a set of initial conditions (lower-boundary conditions) is required to begin the integrations. The particular set of initial conditions discussed here is that required by the Huebsch cloud-rise model which is described in Volume III of this documentation and also in Refs. 1 and 2. These conditions are:

1. The time, relative to detonation time, of the initial-conditions specifications
2. The average temperature of the nuclear cloud at the time of the initial-conditions specifications
3. The total mass of soil material entrained in the cloud and the fractions in vapor and condensed phases
4. Size-frequency distribution of the condensed phase soil material

The initial-conditions specification can account for detonation yields ranging from 0.01 KT to 100 MT, and heights of burst ranging from 1 fireball radius above ground to 20 scaled feet below ground. Two soil types are considered: siliceous and calcareous. Implicit in the specification of the initial conditions is the realization that entrained soil material provides essentially all of the mass of fallout deposited locally. This material is made radioactive principally by occlusion of weapon debris material.

Some additional details of the determinations of these initial conditions are presented in Ref. 3 which is the final report of a program carried out at Tech/Ops to provide the initial-conditions data set. The results of other work done also at Tech/Ops — specifically in revising the initial temperatures and in determining the fraction of the soil burden in the vapor state — are reported here only. We should mention that an additional set of initial conditions obtained from observed cloud-rise data, such as initial cloud dimensions and velocity, is to be found in Refs. 4 and 5.

DETERMINATION OF THE INITIAL CONDITIONS

To supply the initial conditions by means of a theoretical analysis starting from first principles would require an effort far beyond both the fiscal and temporal scope of the program funded for this work. In addition to the need for a detailed theoretical description of the complex events and interactions during and following a nuclear explosion, a very large scale computing effort would be required to provide a sufficiently complete time history of the fireball and early cloud development. The analysis would need to cope with a two-phase environment (air and ground) in such fine detail and over such a long period of time as to transcend the current state-of-the-art in the field. Because of the physical complexity and large scale of a nuclear detonation, it is doubtful that less exacting theoretical calculations could produce meaningful results. Attempts have been made in the past to provide the required information using simplified theoretical models, but in the end so many questions were left unanswered that one must be extremely skeptical about the accuracy of the results. We concluded that our best recourse was to make use of field data observed at nuclear tests.

Needless to say, utilization of field data does not solve all our problems. In fact, the problems are so numerous and involved that a thorough discussion of them would not be possible within the space requirements of this report. Many of these are discussed briefly in the sections that follow; a few of the larger problems that are only indirectly treated later are as follows: There has not been a really large number of nuclear detonations, and detonations always have occurred under restrictive conditions. For example, U.S. test shots of interest to fallout studies have occurred in only two environments: the Nevada Test Site and the Pacific Testing Grounds. The former has a desert environment; the latter, a tropical ocean environment. All of the large-yield shots have taken place in the Pacific whereas most of the small-yield shots have occurred in Nevada. Most of the Nevada shots have been air bursts or tower bursts which produced little or no local fallout. At only a few shots have fallout-study programs been carried out on a scale large enough to yield comprehensive results; several of these studies were done in the Pacific in connection with multi-megaton detonations that scattered fallout over

such large areas of ocean that only sparse samplings could be taken. There are essentially no applicable data for the lowest end of the yield range, and, of course, no known shots have been as powerful as those at the highest end.

On the other side of the coin, we have been fortunate in having available several sets of extremely useful data. Particularly noteworthy are the unpublished cloud rise and growth data of Edgerton, Germeshausen and Grier, Inc.,⁶ the temperature data of Hillendahl,⁷ the crater-scaling equations developed by Nordyke,⁸ the fallout data collected from shots TEAPOT Ess⁹ and SUN BEAM Small Boy,¹⁰ and the DASA compilation of fallout data.¹¹

Time of Initial Conditions Specifications

The first step in establishing a set of initial conditions is to select an appropriate time at which the initial conditions are to be specified. Various alternatives are available. For example, we could select the detonation time, but then we would necessarily have to include in our subsequent analyses and computational simulations the very early phenomenology of the radiative fireball growth in addition to cloud rise and growth. A second alternative would be to select the time at which a particular temperature is reached. This alternative is particularly attractive because one might pick a temperature at which it is certain that all of the entrained soil material has condensed. Obviously, this simplifies the ensuing cloud-dynamics calculations and, even better, it eliminates the troublesome problem of establishing the fraction of the soil burden in the vapor state. Another convenient temperature might be one that is critical in the partitioning of activity between refractory and volatile radioactive isotopes. This would link the initial-time determination with the activity fractionation process. Actually, we have used none of these alternatives.

In choosing a time for the initial-conditions specification, one should not lose sight of the primary purpose in supplying the initial conditions: namely, to provide a set of lower-boundary conditions for use by a dynamic cloud rise and growth simulation. With this purpose in mind, a study of available cloud rise and growth data derived from movie films of test shots⁶ readily reveals an appropriate time. However, to thoroughly understand the significance of the time selected, a brief discussion of the cloud data in terms of the dynamics of cloud rise and growth is warranted. Figure 1 illustrates typical plots of cloud dimensions versus time.

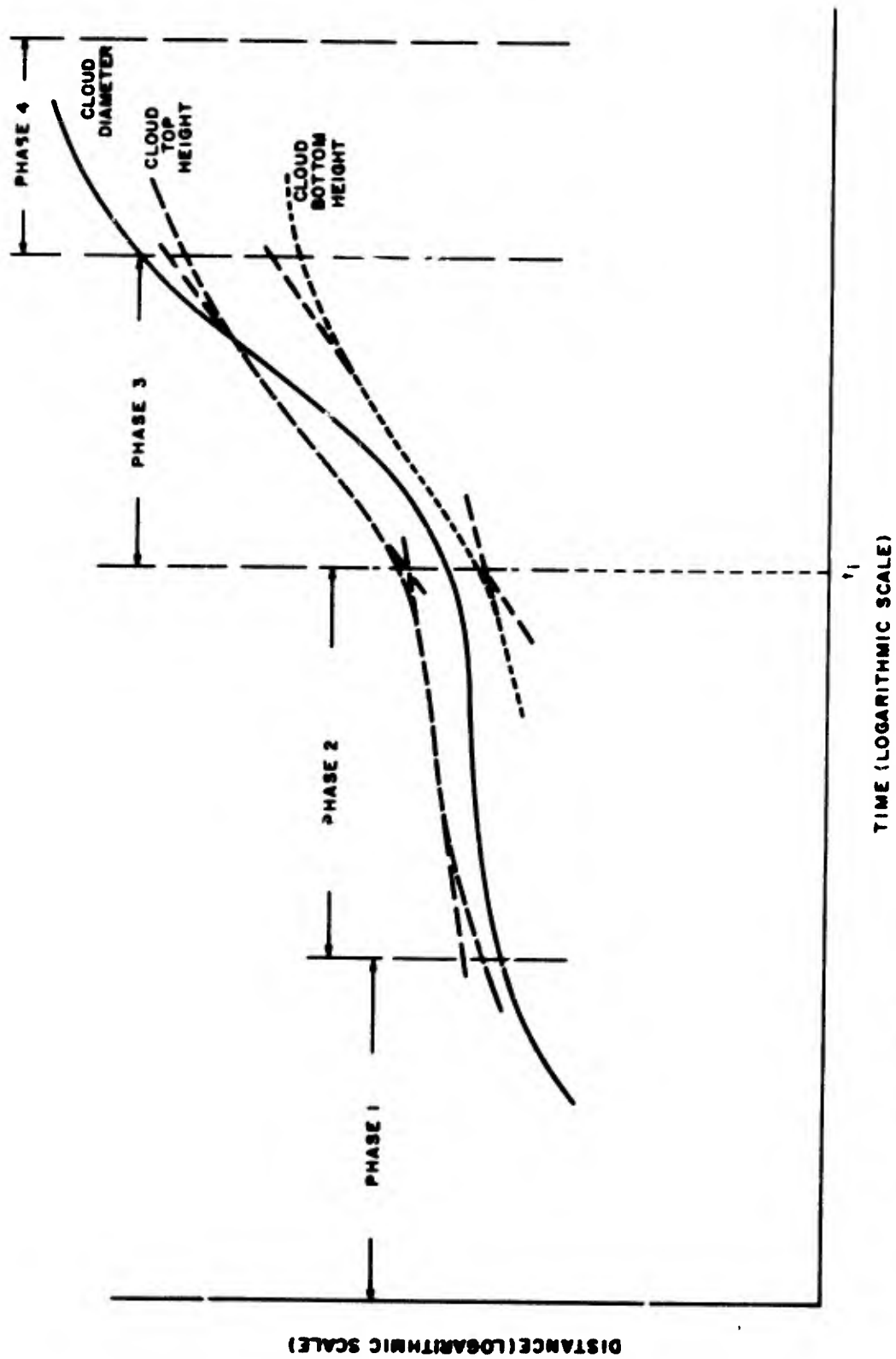


Figure 1. Typical Cloud Dimension Plot vs. Time (The four phases of cloud development and time of initial-conditions specification, t_1 , are also shown.)

We have found it convenient and appropriate to divide the development of a nuclear cloud into four phases. These are (in temporal sequence):

1. A fireball phase
2. A pseudohydrostatic cloud rise phase
3. A similarity cloud rise phase
4. A final expansion phase leading to stabilization.

The fireball phase covers the interval from the detonation time until radiative growth of the fireball has virtually ceased and pressure equilibrium with the atmosphere surrounding the fireball has been achieved. The prompt effects, including the electromagnetic pulses and the close-in blast, have largely subsided by the end of this period. During phase 2, the fireball is still hot (in fact, the second temperature maximum usually occurs early in this phase), but not hot enough for radiation to dominate the cooling process. Graphs of fireball center height versus time indicate decelerative rise. Because of vigorous vortex circulation, the fireball entrains appreciable amounts of ambient air; this causes rapid cooling. The entrainment rate during phase 2, though significant, is substantially less than the rate that occurs subsequently and, in comparison with this later behavior (phase 3), the cloud behaves more like an air bubble rising in water.¹² For this reason we have labeled it the pseudohydrostatic rise phase. The comparatively low entrainment rate probably is caused by the fact that the cloud temperature is sufficiently high, and as a consequence, the difference in density between the cloud gases and the ambient air is sufficiently great ($\rho_{\text{ambient}}/\rho_{\text{cloud}} > 10$), to prevent an effective momentum transfer from the circulating cloud gases to the ambient air. An interpretation of this type has been presented previously by Batchelor.¹³

A short period of accelerative cloud center rise appears to occur in a small time interval centered on the boundary between phases 2 and 3. Subsequent to this period, during phase 3, decelerative rise and growth is resumed. An appreciation of the critical influence of vortex circulation on cloud rise and growth is required for an understanding of these processes. Figure 2 shows an artist's conception of the geometry and structure of organized vortex circulation within a nuclear cloud. (Detailed discussions of the physics of vortex rings and the efficacy with which vortex ring geometry and circulation fit observed nuclear cloud behavior have been presented

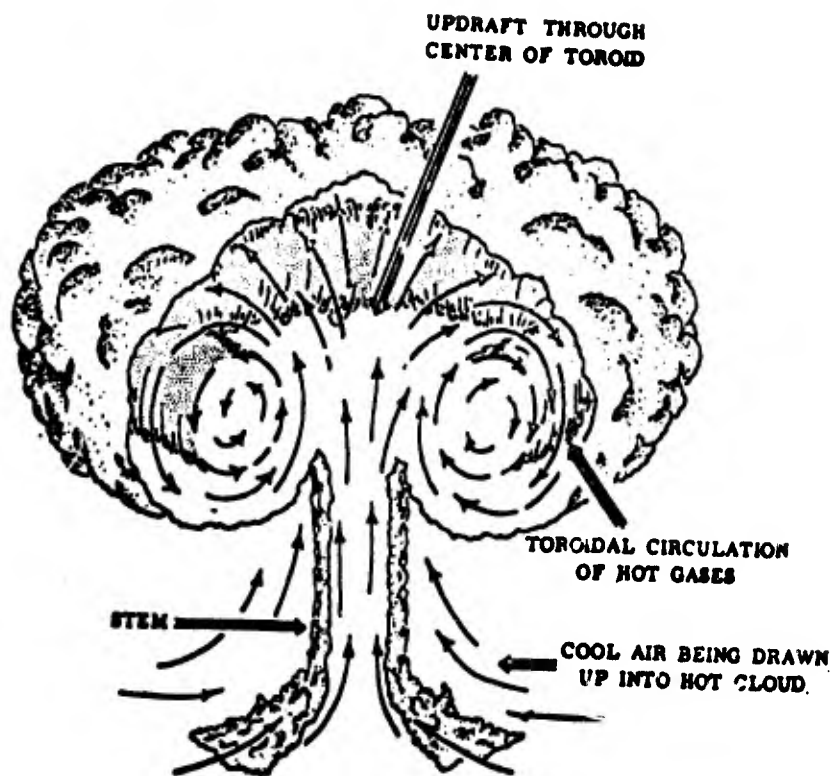


Figure 2. Toroidal Circulation Within a Nuclear Cloud (From Ref. 14)

by Normant.^{15, 16} Movie films of nuclear clouds show that during phase 2 this circulation is very vigorous but, as noted earlier, because of the gross density difference between the cloud and ambient gases, there is little effective transfer of circulatory momentum from the cloud to the surrounding air. However, at approximately the time of the beginning of phase 3 the combined influence of the lowered temperature and the circulation vigor are sufficient to cause more effective momentum transfer. When this occurs, the vortex circulation causes increasingly vigorous expansion of the cloud into the surrounding air. This dynamic interaction, which causes much higher rates of cloud growth, continues throughout phase 3. The rise and growth are correlated during phase 3 in such a manner that geometric similarity of cloud shape is maintained approximately. That is to say, if we view the cloud as an oblate ellipsoid, the ellipsoid eccentricity does not vary greatly during phase 3.

Subsequent to phase 3, cloud behavior is dependent on weapon yield and height of burst. For small detonations at low altitudes, rise momentum and circulation subside at a level below the tropopause. For large detonations, the tropopause

is encountered during the cloud rise and the cloud passes into the stratosphere where the ambient temperature actually increases with altitude. This so-called "temperature inversion" results in a rapid loss of cloud buoyancy and causes the cloud rise to cease while circulatory motion (vorticity) continues to persist. The residual vorticity then is dissipated by lateral expansion while the cloud height remains fixed.

Obviously, the largest amount of the cloud rise and growth occurs during phase 3. Furthermore, currently available cloud-rise models are applicable only as early as the beginning of phase 3. Therefore, we have chosen the beginning of phase 3 as the most appropriate time for specification of initial conditions.

The initial time, t_1 , was found by extending the straight portions of both the cloud-top-height and cloud-bottom-height curves during phases 2 and 3 to their points of intersection, as shown in Figure 1. Then the ratios t_1/t_{2m} , where t_{2m} is the time of the second temperature maximum, were plotted against yield. Data for 14 shots ranging in yield from 1.2 KT to 15 MT were included in the plot.³ Whereas there is considerable scatter in the observed data, there is a definite trend that indicates clearly an approximate power law relationship. This relationship was determined by least squares to be

$$t_1 = 56 t_{2m} W^{-0.30} , \quad (1)$$

where W is in kilotons. No height of burst effect is apparent in the data.

Values for t_{2m} can be computed from the equations of Hillendahl.⁸ For air bursts,

$$t_{2m} = 0.045 W^{0.42} ; \quad (2)$$

for water surface bursts,

$$t_{2m} = 0.037 W^{0.49} , \quad (3)$$

where W is in kilotons and t_{2m} is in seconds. The necessity for segregating Hillendahl's observed data in groups of air bursts and surface bursts and determining an individual equation for each set is discussed on p. 62 of Ref. 3. These equations can be combined by linearly interpolating between them to yield

$$t_{2m} = 0.037 \left[1.216 \frac{\lambda}{180} \right] W^{(0.49 - \frac{0.07\lambda}{180})}, \quad -20 \leq \lambda \leq 180 \quad (4)$$

where λ is the scaled height of burst in units of $\text{ft}/\text{KT}^{1/3}$.

The use of Eq. (4) for subsurface bursts has not been adequately justified since appropriate cloud-rise and t_{2m} data are not available for subsurface bursts.

Figure 3 gives computed values of t_i as a function of yield and height of burst

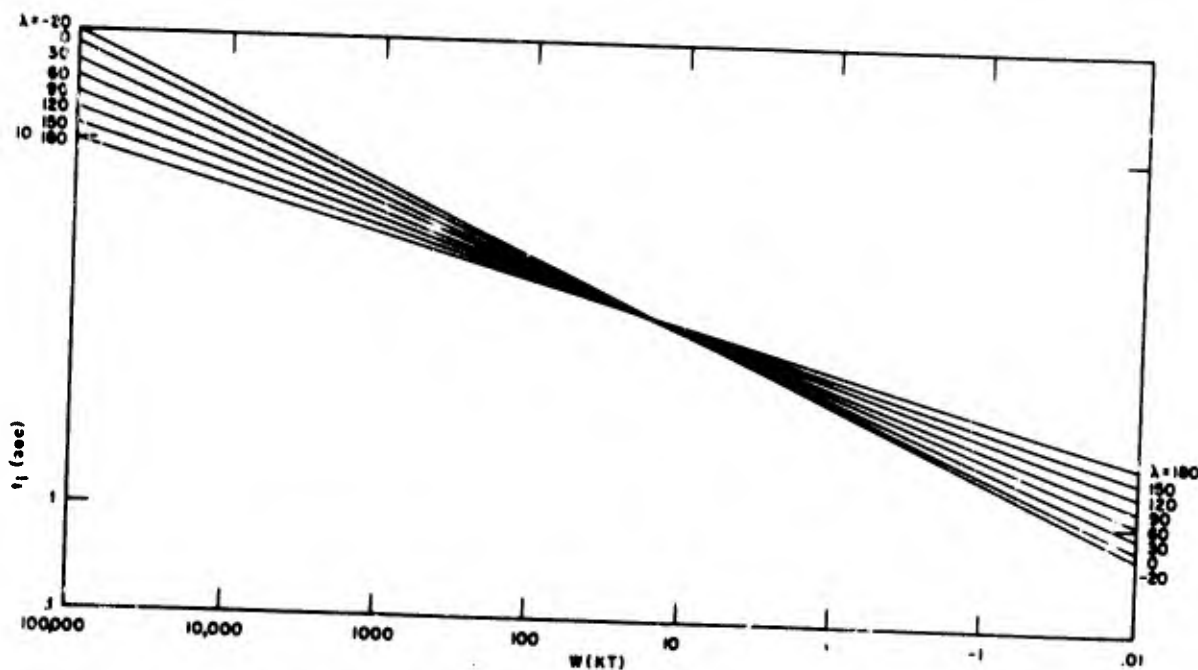


Figure 3. Initial Time vs. Yield as a Function of Scaled Height of Burst

The Initial Temperature

After a particular time at which to specify the initial conditions has been selected, our next task is to estimate an average cloud temperature at that time. We have available both theoretical means and observed data by which to accomplish this. The problem can be attacked theoretically at either of two widely separated levels of sophistication. At the lower level, one can assume a simple partitioning of weapon

energy yield between blast and shock, prompt radiation, nuclear energy, and energy used in heating and lifting the fireball. The cloud temperature at the time of interest is then determined from the residual energy after accounting for all the losses. Moulton¹⁷ has pointed out, however, that because of complex interactions between these processes, simple energy partitioning is not physically meaningful. Furthermore, even if the partitioning were possible in principle, inevitably there would be large uncertainties in each term of the energy-balance equation. Since the information we seek is obtained from differences between energy terms with large uncertainties, we can expect, in many cases at least, that our results will be of the same order as the uncertainties. Such results, then, could not be considered reliable. The theoretical approach at the higher level of sophistication requires numerical solutions of a set of basic hydrodynamic and energy-balance differential equations that can describe the processes in action from detonation time to the time of the initial-conditions specification. The model used would need to cope with the air-ground interface and consequently would have to treat a two-material environment. This type of calculation is grossly demanding of the most advanced computers¹⁸ and would be well beyond both the temporal and fiscal scope of this effort. Fortunately, there are some excellent experimental temperature data observed from fireballs of nuclear test shots, and our best course is to utilize these data.

The experimental data used are Hillendahl's power temperatures listed in Ref. 7. These power temperatures were derived by Hillendahl from observed calorimetric data by using the Stefan-Boltzmann power emission law in the form

$$T = \left[\frac{\pi R^2 \frac{\Delta q}{\Delta t}}{\sigma \epsilon \beta \psi} \right]^{1/4}, \quad (5)$$

where

T = the power temperature

σ = Stefan's constant (1.356×10^{12} cal cm⁻² sec⁻¹ deg⁴)

R = the slant range

Δq = the measured energy in the time interval of length Δt (cal cm⁻²)

β = the weighted cross-sectional area of the fireball observed (cm^2)

ψ = a transmission factor ($0 < \psi < 1$)

ϵ = average emissivity of the fireball surface (taken as 1).

The power temperatures are given as functions of scaled time, i.e., t/t_{2m} , where t_{2m} is the time of the second temperature maximum.

Plots of $\log T$ versus $\log t/t_{2m}$ almost always are linear in the range of scaled time between about 1.1 through 4.0. At larger values of scaled time, the magnitude of the slope often begins to decrease. We have found that individual sets of data can be fitted to an equation of the form

$$T = K \left(\frac{t}{t_{2m}} \right)^n + 1500 \quad (6)$$

A crude theoretical justification for Eq. (6) is given in Appendix A. An illustrative graph of observed and calculated temperatures is shown in Figure 4.

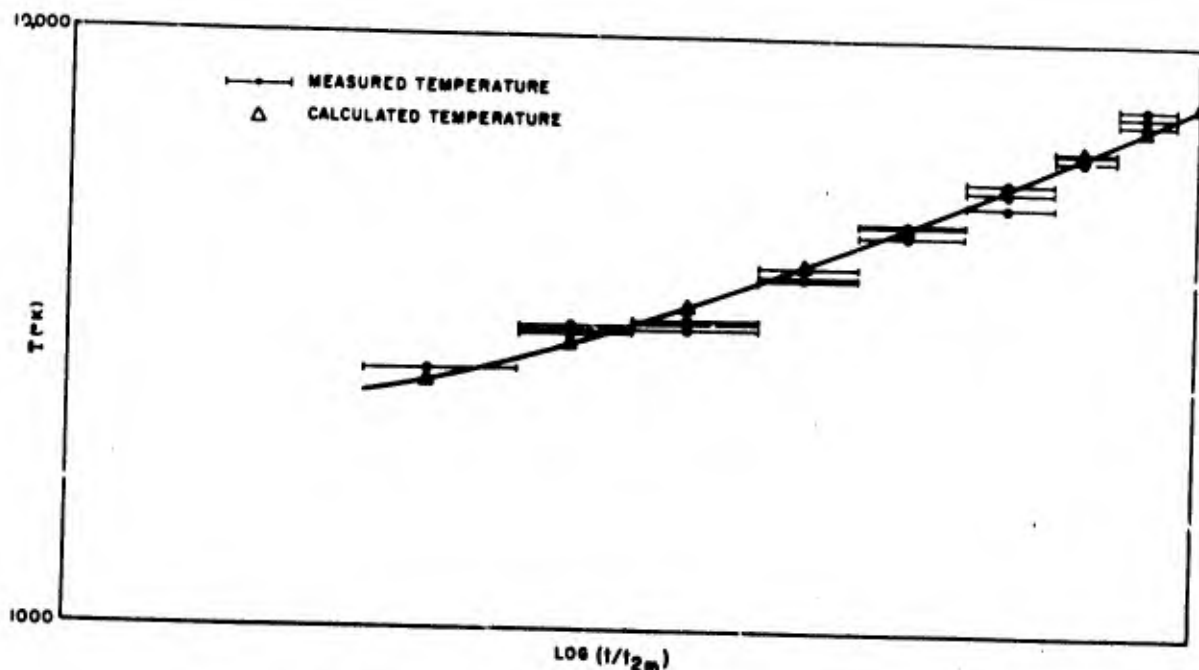


Figure 4. Illustrative Graph of Observed and Calculated Temperature as a Function of Time

Up to this point, the work reported here is the same as that given in Ref. 3; however, since its publication, additional work has been done that has led to a revision of the temperature equations and curves reported in Ref. 3. This additional work was made possible by an independent program of studies at Tech/Ops of observed kinematic cloud-rise data that resulted in determinations of cloud volumes at our initial time as a function of yield and height of burst.* With this new information available we were able to perform energy balance calculations which indicated that our temperatures for low yield surface and subsurface burst were too high. In light of this information, we have reconsidered our analysis of Hillendahl's temperature data as follows.

In our original study, the constants K and n were determined graphically for each of a number of shots. To determine yield scaling for these parameters that is independent of height of burst effects, it was necessary to separate the data into two groups: one for air bursts and the other for surface bursts. Only for these two categorizations are the data sufficiently numerous to permit scaling. Therefore n and K were determined as functions of yield separately for the air bursts and surface bursts. To determine height of burst between these extremes, a linear height of burst interpolation was assumed arbitrarily for both K and n . (Additional details are given in Appendix A of Ref. 3.)

In determining yield scaling of n and K , we observed that the water surface burst data alone yielded relatively clean linear log-log graphs whereas data from land surface (which in all cases included considerable water also) and shielded bursts, while not substantially different from water surface data, tended mostly to increase the scatter on the graphs and thereby add confusion to a situation that already was somewhat obscure. Because of this we used only the water surface data. In reworking the data, we included these "wet" land surface and shielded detonations. These amounted to six additional shots and included one at a much lower yield (about 40 KT) than was available in the initial data set. The augmented data set does not display a clearly defined height of burst effect in the n versus W graphs so that no such effect for n appears in the final equation. The height of burst effect for K remains clearly evident.

* This work was done under the auspices of the Office of Civil Defense for the Naval Radiological Defense Laboratory (Contract N228 (62479) 67712).

The final parameters decided upon did not account for different types of surface material since no unambiguous data are available. (All land-surface bursts in the Pacific incorporated some water.) The linear relationship in λ , assumed for the effect of height or depth of burst, could not be checked because insufficient data exist for tests with scaled burst heights between surface and air bursts, and no information on temperatures is available for underground bursts. The range of yields did not extend to the extremes at the high and low ends of the scale (0.01 KT and 100 MT), so these values are the results of simple linear extrapolations from available data.

The complete expression for calculating the initial temperature given by Eq. (6) is

$$T = K \left(\frac{t}{t_{2m}} \right)^n + 1500$$

in which

$$K = K_0 (k)^{\lambda/180} W^{(\rho_0 + \rho \lambda/180)} \quad (7)$$

and

$$n = n_0 W^{q_0} \quad (8)$$

where

$$K_0 = 5980.$$

$$k = 1.145$$

$$\rho_0 = -0.0395$$

$$\rho = 0.0264$$

$$n_0 = -0.447$$

$$q_0 = 0.0436 ;$$

W is the detonation yield (KT) and λ is the scaled height of burst (ft/KT^{1/3}).

The height of burst and yield ranges of the model are

$$-20 \leq \lambda \leq 180 ,$$

and

$$0.01 \leq W \leq 100,000 .$$

Temperatures obtained from Eqs. (6), (7), and (8) are to be used as average cloud temperatures. Figure 5 shows curves of temperature at t_1 as a function of yield and height of burst.

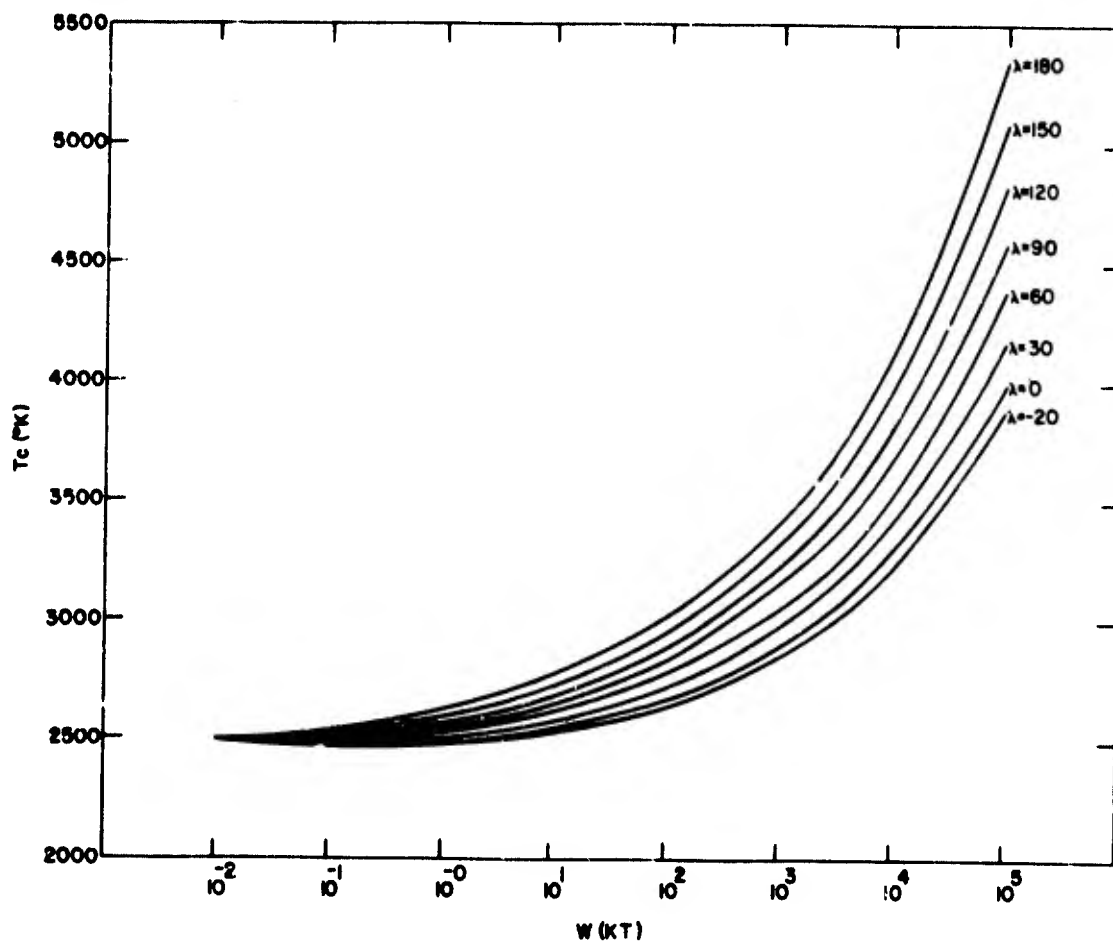


Figure 5. Calculated Cloud Temperature at t_1 vs. Yield as a Function of Height of Burst¹

Soil Loading of the Cloud

Background. When a nuclear detonation occurs at an altitude such that little or no soil material is ingested into the fireball, it is always observed that only minor amounts of local fallout are deposited. This is because the device material is diluted in concentration by being distributed over a very large volume of space in the fireball and therefore tends to condense into small particles. Stewart¹⁹ has estimated that modal-particle sizes would be in the submicron range under such conditions. These small particles remain entrained in the circulating cloud gases and are carried to high altitudes in the "mushroom cap" of the nuclear cloud. Because of their small settling rates, the particles are suspended in air, high above ground, during the period of their greatest radioactivity; then, because of the dispersing action of the atmospheric winds, they are finally deposited over a large area of the earth's surface. For a surface or near-surface burst, on the other hand, a large quantity of finely divided soil material in the fireball provides a large surface area on which the vaporized debris material can condense; in this case the debris material, and its associated radioactivity, become distributed on and through the large soil particles. These large particles rapidly settle to the earth's surface to cover a relatively small area downwind of the detonation. As a result, a high level of activity and a serious local fallout threat are expected. The important point here is that the soil comprises the bulk of the fallout material; in fact, for all cases of interest to us, we shall assume that the mass of device material is insignificant compared with that of the soil and that the soil burden of the cloud is the fallout burden.

Another important aspect of the problem concerns the relation of the mass of the cloud soil burden at the time of the initial-conditions specification to the mass of fallout material deposited locally; the two are often far from equal. Though ultimately we are interested only in the local fallout, we must know the total soil burden at the initial time to properly account for its effects on cloud-rise and to allow for proper distributing of activity. Since the initial time is relatively early in the cloud history (from approximately 1 to 20 sec depending on yield and height of burst) little error is introduced by neglecting losses from the cloud at earlier times.

It is evident that the prime factors influencing the soil loading of the fireball are the yield and height (or depth) of burst of the nuclear device. In addition, the characteristics of the medium in which the device is detonated, the topography of the blast site, and the nature and quantity of other materials in the immediate environment of the blast are factors which also contribute substantially to the final fallout patterns.

There are a number of procedures that conceivably can be used to estimate soil contents of nuclear fireballs. We have chosen to label these methods (1) energy partition, (2) hydrodynamics calculation, (3) cloud buoyancy, (4) back extrapolation, (5) specific activity, (6) crater volume, and (7) fireball volume. We have studied and evaluated each of the methods; discussions of the results of our deliberations are presented in Ref. 3 and, therefore, will not be repeated here. In determining soil loadings for specific test shots and also in deriving yield and height of burst scaling functions we have used methods 4, 5, 6, and 7.

Soil Burden Determinations for Selected Test Shots. In constructing and calibrating our model, we were restricted to a consideration of nine shots whose yields ranged from 1.2 to 15,000 KT, with scaled heights (depths) of burst* extending from $-63.51 \text{ ft} \cdot (\text{KT})^{-1/3.4}$ to $130.152 \text{ ft} \cdot (\text{KT})^{-1/3.4}$. (This restriction to nine shots was dictated by the extent of information available regarding radiological and fallout mass collection data.) For two of the nine shots, the available data are of interest but are not quite appropriate for our needs. Specific activity data for one shot were taken from fallout samples collected on a Japanese fishing boat; their accuracy is open to question. Another case considered is a barge shot over shallow water which consequently cannot properly be classified as a land-surface burst.

We used two methods to reduce the raw data. The first method directly integrates the mass deposited over the local fallout area. Continuous curves of fallout mass per unit area, m , deposited at distances R along radial lines emanating from ground zero were obtained from fallout collection-station data by least squares fitting of the data to a function of the form

* In the soil burden work we have used the scaled height of burst, Λ , defined by Nordyke:⁸ $\Lambda = hW^{-1/3.4}$, where h is the height of burst in feet and W is yield in kilotons. Note that for the time and temperature determinations we have used the scaled height $\lambda = hW^{-1/3}$.

$$\ln(m) = a \ln(R) + b \quad , \quad (9)$$

where a and b are constants that are unique to a particular radial line. Using this function for extrapolation, we were able to construct isomass contours well beyond the actual range of observation, and thereby extend the mass integrations to include virtually all of the local fallout. The derivation of Eq. (9) and a description of the data-reduction method are given in Appendix B of Ref. 3. This method was used for two of the nine shots since only for these two were a sufficient number of collection stations employed. These shots are SUN BEAM Small Boy and TEAPOT Ess. Figure 6 gives the extended isomass contours for TEAPOT Ess (1.3 KT, -67 ft).

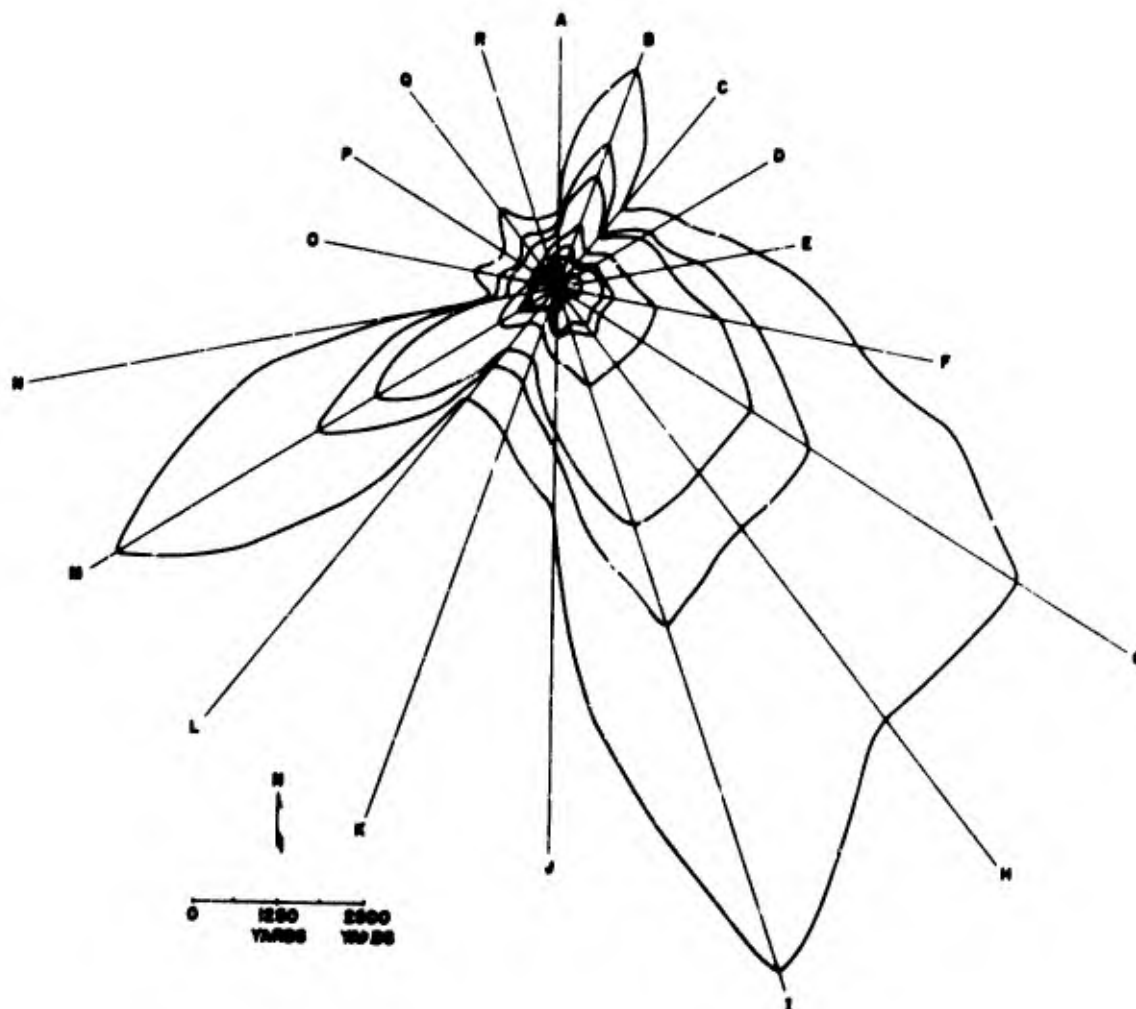


Figure 6. Ess Isomass Contours (The contour levels are 1000, 100, 50, 10, 1.0, 0.5, 0.1 g/ft²)

For three REDWING shots — Tewa, Zuni, and Lacrosse — total soil masses in the clouds were obtained by analysis of specific activity data* that were measured from fallout samples collected for these shots. Specific activities for Ce^{144} were used instead of Mo^{99} data for reasons discussed in Section 4.9 of Ref. 20. Selected data recommended by Mr. R. C. Tompkins, Nuclear Defense Laboratory, from Tables 3.21, 3.24, and 3.25 of Ref. 20 were used. Specific activities, in units of fissions/unit mass of sample, for the remaining four shots were taken from Miller²¹ (Table 3.11); these specific activities were based on Mo^{99} data.

For SUN BEAM Small Boy, radiological data as well as mass deposition data were obtained at the fallout collection stations. This afforded the opportunity to compare masses estimated by the two methods. If we exclude the results from two stations which appear to be spurious, the average mass determined by the specific activity method agrees with the value obtained by integration of the fallout mass deposition data to within 40%.

Major sources of error in the two methods of data reduction are known, but quantitative determinations of the errors are not possible since the total fallout from a nuclear explosion has never been determined. In the method of direct mass integration, the largest error lies in the assumption that the mass measured on the ground contains all the fallout, and thus all the soil mass in the cloud. A sizable proportion of the lightest particles in the cloud settle well beyond the range of the close-in fallout area. In fact, many particles are carried far aloft and contribute to worldwide fallout. This effect is particularly enhanced if the winds above the blast site are strong. Errors of this type are expected to be minimized for underground shots and shots in soil with relatively large soil particle sizes, since we then expect lower cloud heights and faster particle fall rates. A second major source of error is caused by contamination in the collectors. Since fallout areas are too hot to be entered immediately, ambient winds naturally will add dust to some collectors before the samples can be recovered. For SUN BEAM Small Boy, which was

*The specific activity method consists essentially of extrapolating measured specific activities to zero time, conversion from curies/mg of sample to equivalent fissions, and finally division into the total number of fissions produced by the detonation.

exploded over soil in the talc-size range, both sources of error may have seriously biased the observed size distributions. Although TEAPOT Ess was detonated in soil which had larger granules than SUN BEAM Small Boy, there was a base surge which extended out well over a mile from ground zero. The close-in stations therefore may have collected a significant amount of material that could not properly be classified as fallout.

The main source of error in determining soil mass loading of the cloud by activity measurements lies in determining an average value of the specific activity. Specific activity will vary with particle size and location. Since the number of collection stations for the tests for which this method was used were too few to accurately determine the average specific activity with respect to location, we were forced to assume that the measurements actually available were representative of the average specific activities.

Development of Scaling Functions. After the total fallout mass had been determined for the nine cases, two models, one for subsurface and the other for air bursts, were developed to correlate the results with yield and height of burst. We necessarily relied heavily on observed phenomenology associated with nuclear blasts. For surface and subsurface bursts we found it natural to ask whether mass lifted could be correlated with crater volume. We plotted fallout mass versus crater volumes as calculated for a paraboloid-shaped crater (from crater data given in Ref. 11). The graph shows that it is reasonable to suppose that a power-law relationship holds between the mass lifted and the volume of the resulting crater. The slope of the least squares straight line fitted to the data is 0.86. Since the plot is on a log-log scale, this slope implies that to the extent that our data are reliable, we may assert that the mass lifted in a detonation is approximately directly proportional to the volume of the crater produced.

The problem of the yield and depth of burst dependence of the soil loading is now much more tractable since we need look only at the dependence of crater volumes on yield and depth of burst, an area that has been investigated much more thoroughly than that of the fallout mass itself. Specifically, the relationship of crater volume to yield and depth of burst has been investigated in detail by Nordyke.⁸ While the functions he derives are based only on high explosive bursts, his comparison of the

functions with data from low-yield nuclear bursts shows compatibility, the discrepancies in crater dimensions being no more than 10%. One obvious difficulty in calibrating a volume scaling function is the lack of really pertinent data at very high yields. Because of this, and since data on craters produced by high-yield explosions are in general sparse, we have chosen to use Nordyke's scaling functions extrapolated to the high-yield region. Nordyke's functions correlate quite well with the available crater data for the high-yield region. We have, then:

$$M = K_z R^2(z) D(z) W^{3/3.4}, \quad (10)$$

where

M = the total mass of soil in the cloud (g)

W = the yield (KT)

z = the scaled depth of burst (ft \cdot KT $^{-1/3.4}$)

$$R(z) = 112.5 + 0.755z - 9.6 \times 10^{-6} z^3 - 9.11 \times 10^{-12} z^5$$

$$D(z) = 32.7 + 0.851z - 2.52 \times 10^{-5} z^3 + 1.78 \times 10^{-10} z^5$$

and K_z is a constant (discussed later) that relates the crater volumes to soil mass lifted in the cloud.

For height of burst greater than zero, no study has been made of crater volumes comparable to that of Nordyke's for surface and subsurface bursts. Furthermore, crater-dimension data that are available do not correlate with yield in a consistent manner. Therefore, a different scaling model, based on the following rationalizations, was used for air bursts. The most intense blast and thermal effects of nuclear detonations are contained within the region of the fireball, and it is within the reach of this region that the cratering and soil incorporation take place. Of course, the dimensions of the fireball vary with time and never are precisely defined. However, we know that the fireball has a spherical shape, and we can reasonably assume that its volume is approximately proportional to the detonation yield. Therefore, a characteristic dimension of the fireball, for example the radius, will vary approximately as the cube root of the yield, namely

$r \sim W^{1/3}$. (This relation provides the basis for the form of the height of burst and depth of burst-scaling functions, $\lambda = hW^{-1/3}$ (Ref. 14, sections 3.55-3.58), or $\Lambda = hW^{-1/3.4}$ (Ref. 8).) If the cratering and soil incorporation occur within reach of the fireball, it is reasonable to expect that the mass of soil lifted will be proportional to the volume of the fireball segment that appears to be intersected by the ground (see Figure 7).



Figure 7. Intersection of a Fireball with the Ground

Our equation for estimating soil mass lifted by a nuclear cloud has the form of the equation for the volume of a segment of a sphere. This segment may be thought of as that portion of fireball volume that is intersected by the ground. In our equation the effects of yield and height of burst are expressed in the combined form of the scaled height of burst Λ . Figure 7 shows the pertinent geometry for a fireball with radius r and with its center at an altitude h above the ground. The hatched area represents the region of the fireball that intersects the ground, the volume of which is given by

$$V = \frac{\pi}{3} (r - h)^2 (2r + h) \quad (11)$$

To specify a particular value for r , and at the same time provide a relationship between h and W that imposes a properly scaled limit on h above which no local fallout can occur, we note (Ref. 14, Section 2.118) that local fallout occurs only when the relation

$$h < 180W^{0.4} \quad (12)$$

is approximately obeyed. This relation provides us with an appropriate exponent to use on the yield in our scaling function; however, to be consistent and to ensure continuity at the ground surface between the scaling functions for subsurface and air bursts, we have chosen to continue to use $W^{1/3.4}$. Now, we define a radius-scaling function by

$$r = 180 W^{1/3.4} \quad (13)$$

In terms of the scaled height of burst and radius-scaling functions, Eq. (13) becomes

$$V = \frac{\pi}{3} W^{3/3.4} (180 - \Lambda)^2 (360 + \Lambda) \quad (14)$$

Thus we obtain finally

$$M = K_{\Lambda} W^{3/3.4} (180 - \Lambda)^2 (360 + \Lambda) \quad (15)$$

The constants K_z of Eq. (10) and K_{Λ} of Eq. (15) were determined as follows. We noted that of all detonations studied, the mass data for TEAPOT Ess are by far the most reliable. Therefore, we used this single shot to calibrate the models. K_z was determined by direct solution of Eq. (10). Then, to satisfy the requirement of continuity at $z = \Lambda = 0$, we set Eqs. (10) and (15) equal and thereby obtained K_{Λ} . In light of the relative unreliability of the remainder of the observed data, this means of calibration is at least as valid as any other that might be proposed. Figure 8 shows calculated masses as a function of yield and height of burst.

The main justification for our models is the agreement between the calculated and the measured data. It is interesting to note that the Stanford Research Institute²² experimentally determined that masses of soil lifted were proportional to crater volumes for a series of low-yield surface shots which they examined. They also determined that crater volume is proportional to yield to the 0.92 power which is in close agreement with our yield to the $3/3.4 = 0.88$ power. Also, since the work reported here was completed, results of a somewhat similar study at the

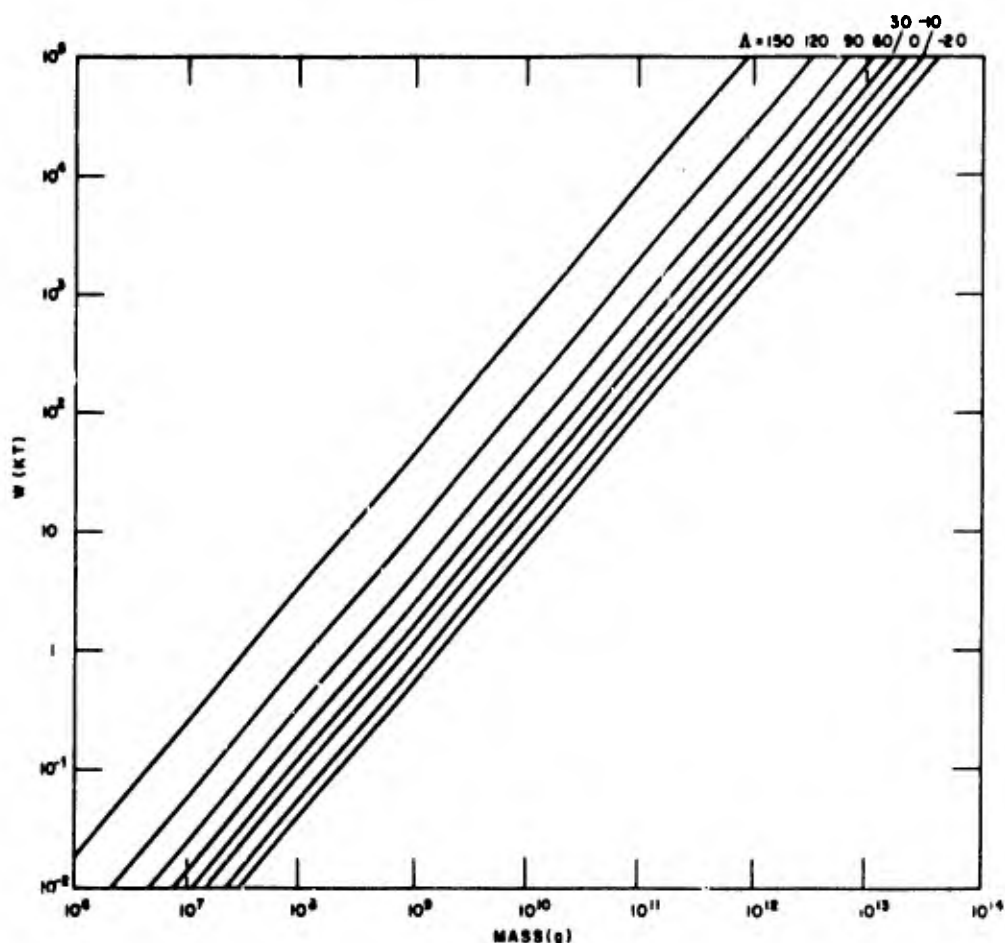


Figure 8. Calculated Total Soil Mass Lifted by the Cloud as a Function of Yield for Various Scaled Heights of Burst

Lawrence Radiation Laboratory have been released.²³ Total masses of soil material carried in clouds for a number of CASTLE and REDWING shots were determined by radiochemical analyses of samples collected by aircraft traverses through the clouds. For the four cases where these data can be compared directly with ours, mass ratio (ours/theirs) is 0.7 for the best case and 27 for the worst.

The complete set of equations governing the soil burden model are as follows:

$$M_{\text{Soil}} = K_z W^{3/3.4} R^2(z) D(z), \quad 0 \leq z \leq 20$$

$$M_{\text{Soil}} = K_A W^{3/3.4} (180-A)^2 (360+A), \quad 180 \geq A \geq 0$$

where

M = the total mass of soil in the cloud (g)

W = the yield (KT)

Λ = scaled height of burst (ft/KT^{1/3.4})

z = scaled depth of burst (ft/KT^{1/3.4})

$R(z) = 112.5 + (7.55 \times 10^{-1})z - (9.6 \times 10^{-6})z^3 - (9.11 \times 10^{-12})z^5$

$D(z) = 32.7 + (8.51 \times 10^{-1})z - (2.52 \times 10^{-5})z^3 + (1.78 \times 10^{-10})z^5$

$K_{\Lambda} = 77.41 \text{ g/ft}^3$

$K_z = 2182 \text{ g/ft}^3$

Phase Partitioning of the Soil Burden. In addition to the average cloud temperature and the total soil burden of the cloud, certain other information is essential to properly account for subsequent cloud rise and growth, distribution of activity among the particles, and the atmospheric transport of fallout. The thermodynamic cloud-rise computations must have the quantity of soil material in the vapor phase and the average temperature of condensed phase material. A knowledge of the fallout particle size-frequency distribution is essential to both the distribution of activity on the particles and atmospheric transport computations. To produce high quality estimates of the quantities mentioned would require an extensive combined theoretical and computational effort that would start from first principles and follow the many relevant complex processes from essentially shot time until the early cloud development. Such an effort never has been undertaken.

These particular problems are complicated by several considerations. At the time of interest, t_1 , there is every reason to believe that a nuclear cloud has a grossly nonuniform structure with respect to soil content and temperature. Of particular significance is the sharp temperature gradient known to exist in the cloud. The cloud is very hot in the region of the ring through the cloud about which the toroidal circulation is centered. Beyond this region in all directions, temperature falls off rapidly with distance. One would expect to find essentially all of the radioactive device debris in the hot region of the cloud. Also, within this region one would expect to find whatever vaporized soil material is in the

cloud. As the cloud rises, this hot material continues to expand into its surroundings and, thereby, to heat and contaminate additional soil. In light of this description of the cloud structure it is apparent that actually it is inappropriate to use temperature and soil concentrations obtained by simple averaging over the total cloud volume. Also of importance here is the expectation that much of the soil burden in the hottest region of the cloud will not be in equilibrium contact with the hot gases there; in other words, we can expect a considerably lower average temperature to prevail for soil than for the gases in the cloud.

From Figure 1 it can be seen that immediately subsequent to t_1 the cloud begins to rise upward rapidly. A strong updraft is produced in the wake of the cloud, and soil dust suspended in air is sucked upward in the stem toward the cloud cap. The vortex circulation in the cloud^{15, 16} is such as to cause very high upward circulation velocities to occur around the center axis of the cloud torus. This tends to pull some stem material into the bottom of the cloud and hence to incorporate this material into the outer cloud layers. This means that the cloud soil burden probably is incomplete at precisely t_1 . We can expect, however, that the burden is completed very shortly thereafter. Unfortunately, there are not available quantitative data on internal cloud structure at times as late as those of interest here, nor do we know how much, if any, soil is incorporated into the cloud after t_1 .

In the paragraphs that follow and in Appendix B, we present the results of tentative estimates for the fraction of the soil burden vaporized and the temperature of the condensed phase soil. This work was done after publication of our initial conditions final report³ because additional information on cloud properties had become available, as mentioned earlier. Specifically, we have determined cloud altitudes and dimensions as a function of yield and height of burst at the initial time. This allows energy balance calculations to be made and we have applied these considerations to a determination of the desired quantities. We repeat that the information sought frequently is lost in the uncertainties that arise because of the approximations used to describe the energy partition model. The results are in a very real sense arbitrary, since by making different basic assumptions in the energy model, very different results can ensue. Furthermore, we must note

that of all possible plausible energy partition models, we have had the opportunity to investigate only one; fortunately this model does give physically reasonable results. Before proceeding into a discussion of the energy balance calculations let us consider some of the general properties of the system.

There are two categories of surface or soil material to be considered: siliceous and calcareous. Characteristic examples of siliceous soil are the common sandy and clay soils. In the case of sand, the chemical composition is almost pure silicon dioxide (SiO_2). For the much more abundant clays, the composition is more complex and there are significant quantities of a variety of metals such as aluminum and iron; but even for clays, the major chemical constituent is silicon dioxide. An average composition for igneous rock, from which the common clays are derived, is:²⁴

<u>Constituent</u>	<u>Percent Weight</u>	<u>Constituent</u>	<u>Percent Weight</u>
SiO_2	60.18	CaO	5.17
Al_2O_3	15.61	Na_2O	3.91
Fe_2O_3	3.14	K_2O	3.19
FeO	3.88	TiO_2	1.06
MgO	3.56	P_2O_5	0.30

We see that the major constituents of clay soil (at high temperatures) are silica and alumina. Thermal properties for these materials are:^{25, 26}

<u>Compound</u>	<u>Melting Temperature (°K)</u>	<u>Boiling Temperature (°K)</u>
SiO_2	2000	3070
Al_2O_3	2323	3773

Common examples of calcareous surface materials are limestone and coral. These substances are essentially calcium carbonate (CaCO_3). However, at relatively low temperatures, calcium carbonate loses carbon dioxide gas to yield a

refractory residue of calcium oxide (CaO). Therefore, in considerations of calcareous material at high temperatures, we use the properties of calcium oxide; melting temperature 2853°K and boiling temperature 3123°K .²⁶

We see then that the minimum boiling temperatures of siliceous and calcareous soils are approximately 3000°K and 3100°K , respectively. Figure 5 shows that cloud temperature at t_1 sometimes is less than the boiling temperatures of the soil material. In such a case we simply take the fraction of soil in the vapor phase to be zero.

In estimating limits on the fraction of vapor phase soil for those cases where the cloud temperature is above that of the soil boiling temperature, we use the following realizations:

1. Temperatures in the cloud above the soil boiling temperature are localized to the region of the vortex ring core.
2. This (thermally) hot region of the cloud contains virtually all of the cloud radioactivity.
3. For surface bursts a large portion of fallout is derived from unvaporized soil particles on which radioactive weapon debris material condenses.
4. The amount of soil vapor in the cloud will be less than the mass of active fallout produced by the detonation.

We assert that item 4 follows from items 1, 2, and 3. At t_1 the vaporized weapon debris material (which has a negligible total mass compared with the total soil burden mass) resides in the hot core ring of the cloud along with the vaporized soil. Both the debris material and the vaporized soil subsequently condense on solid or liquid soil particles to produce the radioactive portion of the cloud soil burden. Obviously the fallout material must include a significant amount of material that was never vaporized in addition to essentially all of the vaporized soil material. Therefore, the fraction of the total fallout mass that is found to be radioactive must exceed the fraction of vaporized soil in the cloud.

A survey of the literature to determine mass percent of active material observed in fallout has revealed that most of the mass and most of the activity are associated with particles in the large particle size range of the size-frequency distribution. For this reason, and since on the average there is only a slight tendency for specific activity of gross fallout to change with particle size, we shall concentrate our attention here on the larger particles. Table 1 is a summary of the best data available for large particles. We see that an average of approximately 50% of gross fallout mass is associated with active material. Therefore, on the basis of the reasoning presented above, we can state with a reasonable degree of confidence that, on the average, less than 50% of the total soil burden is vaporized.

TABLE 1
SELECTED MASS AND ACTIVITY DATA FOR LARGE PARTICLES

Operation Shot	Particle Diameter Range (μ)	Approx. Mass of Total Fallout in Size Range (%)	Approx. Mass of Total Fallout Associated with Active Material in Size Range (%)	Source of Data
REDWING Zuni	> 420	75	75	Ref. 20 Fig. 3.53-3.55 Table 3.17
REDWING Tewa	> 210	90	75	Ref. 20 Fig. 3.57-3.59 Table 3.19
JANGLE Uncle	> 210	—	15	Ref. 22 Table IV (Station E)
SUN BEAM Small Boy	200-1000	58	27	Ref. 27 Table 8.2*
SUN BEAM Johnie Boy	> 200	80	50	Ref. 28 Table 3.17
AVERAGES		76	48	

* Only data from collection stations in the heavy fallout area were considered. These were stations 305, 405, and 503.

To be able to determine a more definite value for the fraction of the soil burden vaporized, and at the same time estimate the temperature of the condensed phase material, we have employed an energy partition analysis of the detonation. The critical problem in our analysis is to determine the fraction of the total detonation energy release that is consumed in heating and vaporizing soil. Since we already have relatively accurate knowledge of cloud altitude (therefore, pressure), cloud volume, temperature of the cloud gas, and total soil burden, a knowledge of energy available for heating and vaporizing soil allows estimates of the temperatures of the cloud contents to be made (see commentary on pp. 8 - 9).

Estimates of energies available for heating soil^{*} were obtained by differencing the thermal energies radiated by air and surface bursts.²⁹ In Ref. 29 the thermal energy radiated is given as a function of yield for both air and surface bursts. With this maximum amount of energy available, it is a relatively simple matter to determine the desired quantities so that energy is conserved. The details are given in Appendix B. The results obtained are as follows:

1. 1.5% of the soil burden is vaporized per 100° excess of the initial temperature (as calculated from Eqs. (6), (7), and (8) over 3000°K for siliceous soils and 3100°K for calcareous soils.
2. The temperature (°K) of the unvaporized soil is given by

$$T = 50 \log_{10} W + 1400$$

where W is the detonation energy yield in kilotons.

Particle Size Frequency Distribution

The problem of determining particle size-frequency distributions at t_1 is essentially the problem of determining the extent to which the preshot soil size-frequency distribution has been altered by the processes of evaporation and growth. In these considerations we can make a broad distinction between the high-yield and low-yield shots. We will consider high-yield shots first. At times prior to t_1 , the fireball is extremely hot (see Figure 5) and because of the stable nature of the vortex circulation, which during the early stages of the cloud development tends to

^{*}There may exist other means for estimating the available energy that are at least as plausible and can give different results.

insure that circulating material will remain contained within a limited region of the cloud, we can expect residence times of entrained material in the hot core to be long enough so that virtually all of this material will be completely vaporized. Beyond this region, condensed phase material should have essentially the preshot soil size-frequency distribution. Subsequent to t_1 , additional soil may be entrained into the cloud; of course this also will have the preshot soil size-frequency distribution. Subsequent to t_1 we can expect growth to occur mainly by two mechanisms: (1) by condensation of vapor onto soil particles, and (2) by agglomeration of melted or partially melted soil particles. For high-yield shots we can expect both of these mechanisms to yield significant growth. The condensed phase material present as early as t_1 , however, would be expected to have essentially the preshot soil size-frequency distribution.

For small detonations we note from Figure 5 that the "average" temperature at t_1 is below the boiling temperature of the soil material. We must assume, therefore, that there is essentially no soil vapor present at t_1 . Also we note from Figure 3 that for the small detonations, t_1 is small; in other words, the time scale of events is greatly compressed for small detonations. This means that there is much less time available for thermal equilibrium between soil and cloud gases to be reached. We hypothesize, and this is supported by energy conservation calculations, that relatively little soil is ever vaporized in small detonations; consequently, there cannot have been significant particle growth by condensation from the vapor. Furthermore, since growth by agglomeration is a slow process, and the cloud cooling rate is very fast in relation to it (as shown by cloud rise simulation calculations), we conclude in light of the compressed time scale that growth by this mechanism also is not significant.

In summary, we find that the preshot soil size-frequency distribution is an adequate approximation to the size-frequency distribution of condensed phase material in the cloud at t_1 . As a corollary to this finding, we anticipate that substantial particle growth occurs only for large-yield detonations.

TABLE 1
A SUMMARY OF PROGRAM FUNCTIONS

PROGRAM NAME	CALLING PROGRAM	FUNCTION
LINK1	--	EXECUTIVE: READ DATA FROM INPUT TAPE, CALL COMPUTATION SUBROUTINES, PRINT THE RESULTS OF INITIAL CONDITIONS COMPUTATIONS, AND TERMINATE PROPERLY BY EITHER CALLING LINK1 OR MERELY STOPPING.
TIME	LINK1	DETERMINE THE TIME OF INITIAL CONDITIONS SPECIFICATION.
TEMP	LINK1	DETERMINE TEMPERATURES OF VAPOR AND UN-VAPORIZED SOIL.
MASS	LINK1	DETERMINE SOIL LOADING OF CLOUD.
VAPOR	LINK1	DETERMINE MASS OF SOIL VAPOR IN THE CLOUD.
DISTR	LINK1	SET THE PARTICLE SIZE DISTRIBUTION PARAMETERS, MEAN AND STANDARD DEVIATION, IF REQUIRED.

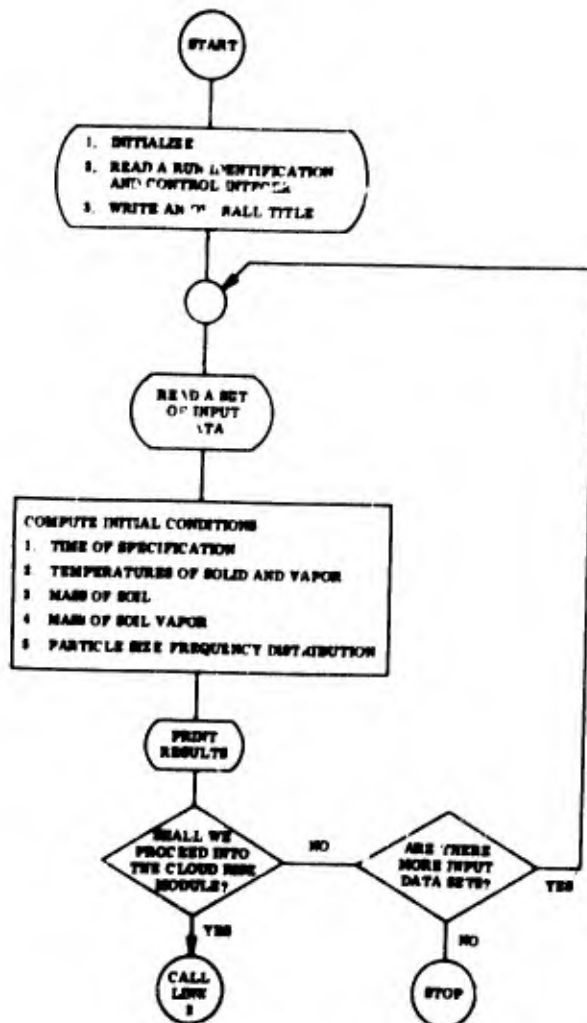


Figure 9. Flow Chart of the Initial Conditions Module Computer Program Logic (LINK1)

COMPUTER PROGRAM OUTLINE

Description

The Initial Conditions Module computer program consists of a main program and five computation sub-routines. Table 2 summarizes the names and functions of these programs. Figure 9 is a general flow chart of this group of programs. Because of the great simplicity of the programming, more detailed flow charts have not been prepared. Instead, the discussion that follows is provided to supplement the FORTRAN card listings. In its initial form, the DELFIC system is designed for execution on the IBM 7094 computer via the IBSYS-IBJOB processor, and the "overlay" feature is used to control the input sequence of major sections of the system. To facilitate discussions of the programs, the executive programs of each major section are assigned names; the Initial Conditions Module executive program is called LINK1. (See Figure 3 of Volume I for a complete presentation of the executive program designations.)

Program Discussion

The Initial Conditions program is designed to serve two objectives. First, it can be used to merely compute and print the values of initial conditions

parameters for an unlimited number of input data sets. Second, it can compute a single set of initial parameter values and then call the next program (LINK2) of the DELFIC system so that cloud-rise computations can be carried out. We shall now refer to the program listing to see how this is accomplished.

After setting two tape name parameters and initializing the data set counter, NN, the program reads an arbitrary 72 character identifier (card) to be used for identifying the initial-conditions data set. Next, the data set count N is read and an overall title is written. At statement number 20, which marks the beginning of the processing loop, the particle size-frequency distribution specification option parameter, IDISTR, is read. This parameter determines whether a log-normal or arbitrary (tabular) particle size-frequency distribution is to be used. If the latter option is selected, the next datum to be read consists of the mid-range diameter value of the first (with smallest diameter) particle size range entry in the tabular representation of the particle size-mass frequency distribution. Next, a data set is read that specifies yield, height (depth) of burst, soil type, and finally geometric mean and standard deviation for a log-normal distribution, or if a tabular distribution is to be used, the number of entries in the table (the maximum number of entries is 40) followed by the table itself (to be described later). If a log-normal distribution is to be used but the mean and standard deviation data card fields are left blank, the mean and standard deviation are supplied by subroutine DSTBN. Then, the height (depth) of burst is converted from meters to feet and the scaled height (depth) of burst is computed and stored in parameter Z. Next, tests are made to see if the model is appropriate for computing for the specified inputs. If it is not, a comment is made at either statement 156 or 143 and eventually control reaches statement 171. At 171, a test of parameter N indicates whether the run should be continued in order to compute initial conditions for other input data or be terminated. The run is terminated whenever either all data sets have been dealt with or when an error or inapplicability of the model is discovered.

If the tests at statements 63 and 66 indicate the model to be applicable, five computational subroutines — TIME, TEMP, MASS, VAPOR, and DSTBN — are called sequentially. Note that subroutine DSTBN is called only if no preshot

particle-size distribution was specified by the user.* At statement 96, certain needed conversions are made and then a complete exhaustive printing of inputs and outputs is made. Once again control reaches statement 171 and if more data sets are to be processed, a transfer is made back to statement 20.

It should be noted that all input and output parameter values are held in common and, therefore, the communication between the Initial Conditions Module (LINK1) and the cloud rise program (LINK2) can be carried out by merely leaving the LINK1 common intact. Because LINK1 executes so quickly, no storage of intermediate results on tape is necessary.

If the user intends to make use of the particle growth option of LINK2, the Cloud Rise Module, he must specify a particle size distribution for the preshot soil over (or under) which the detonation occurs. If this is not possible, it probably will be necessary to employ a particle size distribution for expected fallout. In this case the particle growth option should not be exercised.

As noted earlier, the user has the option of specifying a log-normal distribution for the distribution, or he can specify an arbitrary distribution in tabular form.† The tabular distribution must be constructed and must be input to the program according to the following prescription. The table is constructed so that each successive mid-range diameter and boundary diameter is $\sqrt[3]{2}$ times its preceding diameter. Mid-range diameters are geometric means of the boundaries. In array WHY(I) the mass fraction for each size range is specified in sequence of increasing diameter. There can be no more than 40 entries in the table. A parameter DMIN also is specified which is defined as

$$DMIN = D_1 / (2 \sqrt[3]{2}) ,$$

where D_1 is the upper boundary diameter of the first size range.

If the user chooses to specify a log-normal distribution, he should specify the geometric mean (microns) and geometric standard deviation (dimensionless) of a particle diameter-number frequency distribution function, and optionally, the parameter DMIN (see the preceding paragraph). In this case DMIN is used only for

* It is strongly recommended that the user supply a particle size-frequency distribution for the preshot soil that is appropriate for the geographical location of his simulated detonation.

† Though provision is included for specification of an arbitrary particle size-frequency distribution, the user must specify a log-normal distribution if he intends to use the current version of the DELFIC Particle Activity Module. (See Volume V of this documentation.)

computing fallout from the cloud during its rise. It is not used for setting up particle inputs to the Transport Module. If DMIN is not specified in the input, a value is supplied by the cloud rise program (see Volume III of this documentation).

Operating Information

Because of the simplicity of this program, the following tabular representation of the input data deck (Table 3) is deemed to provide sufficient operating instructions.

TABLE 3
THE INPUT DATA DECK FOR THE INITIAL CONDITIONS MODULE

Card Sequence and Number	Content	Format
1	Arbitrary 72 character identifier	12A6
2	The number of data sets for which initial conditions computations are desired. If the value of this parameter is zero or negative, a single data set will be expected and after computation of its initial conditions parameters, a transfer will be made to LINK2.	I5
3	Preshot soil size-frequency specification option parameter, IDISTR. A value of 0 selects the log-normal distribution option, whereas a value of 1 selects the tabular distribution option.	I5
IF IDISTR=0 {	4 Yield in kilotons, height of burst in meters, * soil type (1.0 indicates siliceous, 2.0 indicates calcareous), mean diameter of the log-normal preshot particle size-number frequency distribution in microns, and the standard deviation of this distribution (dimensionless). If no values are supplied for the mean and standard deviation, the program will supply them.	5F10.3
	5 Mid-range diameter of smallest particle size class to be used in representing the log-normal distribution (if zero, a value will be assigned by the program).	F10.3
IF IDISTR=1 {	4 Yield in kilotons, height of burst in meters, * soil type indicator (1.0 indicates siliceous, 2.0 indicates calcareous).	3F10.3
	5 Mid-range diameter of the smallest particle size class to be used in the tabular representation of the particle size-mass frequency distribution (see the particle size distribution discussion on p. 32).	F10.3
	6 Number of entries in the particle size frequency table (NDSTR ≤ 40).	I5
	7,8,... Particle size — mass frequency table entries with five entries per card. Each entry represents a mass fraction as discussed on p. 32.	5F10.3
N :	Same as card 3 for the second data set	

* This is height above ground zero. For subsurface bursts, the depth of burst is entered as a negative number.

FORTRAN LISTINGS

The FORTRAN listings are included on pp. 35 through 44.

SAMPLE TEST PROBLEM AND PRINTOUT

On pp. 45 through 46 two test problem printouts are presented: (1) with the log-normal soil particle size distribution option, and (2) with a tabular soil particle size distribution. All inputs are printed along with the output and the output is self-explanatory. Preparation of the input cards is discussed in the Computer Program Outline section.

```

SIBFTC LNK1  LIST,DECK,M94/2                                LNK1  0
SUBROUTINE LINK1                                           LNK1  1
INITIAL CONDITIONS (FIREBALL) MODULE                       LNK1  2
TECHNICAL OPERATIONS RESEARCH  22 SEPT 1966               LNK1  3
C                                                         LNK1  4
C ***** LNK1  5
C                                                         LNK1  6
C PROGRAM TO DETERMINE THE INITIAL CONDITIONS SPECIFICATIONS OF LNK1  7
C TIME, TEMPERATURE, TOTAL SOIL MASS, FRACTION OF THE SOIL BURDEN IN LNK1  8
C THE VAPOR PHASE, AND THE SIZE FREQUENCY DISTRIBUTION OF THE LNK1  9
C CONDENSED PHASE SOIL LNK1 10
C                                                         LNK1 11
C THE FIRST CARD CONTAINS ANY ARBITRARY ALPHANUMERIC IDENTIFICATION LNK1 12
C THE SECOND CARD OF THE DATA DECK CONTAINS THE NUMBER OF CASES TO LNK1 13
C BE RUN, FORMAT (15). LNK1 14
C THIS PARAMETER SHOULD BE LEFT BLANK IF THE USER WISHES THE PROGRAM LNK1 15
C TO CALL LINK2 AND SHOULD BE GIVEN SOME POSITIVE VALUE N IF LNK1 16
C THE USER WISHES THE PROGRAM TO STOP AFTER COMPUTING N SETS OF LNK1 17
C INITIAL CONDITIONS. LNK1 18
C                                                         LNK1 19
C OTHER INPUT PARAMETERS ARE - TEST PARAMETER (IDISTR) TO DETERMINE LNK1 20
C IF THE PARTICLE SIZE FREQUENCY DISTRIBUTION IS LOG-NORMAL OR LNK1 21
C TABULAR, YIELD IN KILOTONS, HEIGHT (DEPTH) OF BURST IN METERS, LNK1 22
C A SOIL TYPE INDICATOR, DIAMETER OF THE SMALLEST PARTICLE SIZE LNK1 23
C (MICRONS), MEAN (MICRONS) AND STANDARD DEVIATION, FOR A LOG-NORMAL LNK1 24
C PARTICLE SIZE FREQUENCY DISTRIBUTION , OR IF A LNK1 25
C TABULAR DISTRIBUTION IS USED, THE MEAN AND STANDARD DEVIATION ARE LNK1 26
C DELETED AND REPLACED BY THE NUMBER OF ENTRIES IN THE TABLE. IF A LNK1 27
C LOG-NORMAL DISTRIBUTION IS TO BE SUPPLIED BY THE PROGRAM, THE LNK1 28
C MEAN AND STANDARD DEVIATION FIELDS ARE LEFT BLANK. LNK1 29
C                                                         LNK1 30
C FOR UNDERGROUND BURSTS INPUT DEPTH OF BURST AS A NEGATIVE NUMBER LNK1 31
C                                                         LNK1 32
C THE OUTPUT UNITS ARE MASS IN KILOGRAMS, LENGTH IN METERS, TIME IN LNK1 33
C SECONDS, TEMPERATURE IN DEGREES KELVIN, YIELD IN KILOTONS, LNK1 34
C DISTRIBUTION PARAMETERS IN MICRONS LNK1 35
C                                                         LNK1 36
C ***** GLOSSARY ***** LNK1 37
C                                                         LNK1 38
C DETID(1) INITIAL CONDITIONS IDENTIFICATION ARRAY LNK1 39
C DIAM MEAN DIAMETER OF PARTICLE SIZE DISTRIBUTION (MICRONS) LNK1 40
C DMIN DIAMETER OF SMALLEST PARTICLE SIZE (MICRONS) LNK1 41
C IDISTR CONTROL INTEGER FOR PARTICLE SIZE DISTRIBUTION LNK1 42
C 0 - LOGNORMAL DISTRIBUTION LNK1 43
C 1 - TABULAR DISTRIBUTION READ IN ON CARDS (ARRAY WHY) LNK1 44
C IS CONTROL INTEGER SPECIFIES WHETHER LOGNORMAL LNK1 45
C DISTRIBUTION IS SPECIFIED BY THE USER OR BY THE LNK1 46
C PROGRAM LNK1 47
C 0 - PROGRAM SPECIFIED LOG-NORMAL DISTRIBUTION LNK1 48
C 1 - USER SPECIFIED LOG-NORMAL DISTRIBUTION LNK1 49
C ISIN SYSTEM INPUT TAPE LNK1 50
C ISOUT SYSTEM OUTPUT TAPE LNK1 51
C N CONTROL INTEGER - NUMBER OF INPUT BURSTS LNK1 52
C NDSTR LENGTH OF ARRAY WHY LNK1 53
C NN INTEGER - TESTS NUMBER OF BURSTS RUN AGAINST THE LNK1 54
C NUMBER OF BURSTS TO BE RUN LNK1 55
C RMIN RADIUS OF SMALLEST PARTICLE SIZE (MICRONS) LNK1 56
C SD STANDARD DEVIATION OF PARTICLE SIZE DISTRIBUTION LNK1 57
C SSAM MASS OF CONDENSED PHASE MATERIAL AT SPECIFICATION LNK1 58
C TIME LNK1 59

```

```

C      TME      TIME OF INITIAL CONDITIONS SPECIFICATION      LNK1 60
C      TMP1     AVERAGE TEMPERATURE OF GAS IN CLOUD          LNK1 61
C      TMP2     AVERAGE TEMPERATURE OF CONDENSED PHASE MATERIAL IN CLOUD LNK1 62
C      T2M      TEMPORARY STORAGE                             LNK1 63
C      U        SOIL CLASS INDICATOR                          LNK1 64
C              1.0 FOR SILICEOUS                              LNK1 65
C              0.0 FOR CALCAREOUS                              LNK1 66
C      VPR      MASS OF VAPOR IN CLOUD AT SPECIFICATION TIME  LNK1 67
C      W        WEAPON YIELD (KT)                             LNK1 68
C      WHY(1)    ARRAY OF FRACTION OF TOTAL PARTICULATE MASS IN I-TH LNK1 69
C              PARTICLE SIZE CLASS. MAXIMUM LENGTH OF ARRAY = 40 LNK1 70
C      X        HEIGHT OF BURST (METERS)                       LNK1 71
C      Z        SCALED HEIGHT OF BURST                         LNK1 72
C              LNK1 73
C      ***** LNK1 74
C              LNK1 75
C      COMMON /SET1/ LNK1 76
C      1      DIAM ,DETID(12),IRISE , IEXEC , ISIN , ISOUT , LNK1 77
C      2      SD , SPAR , SSAM , TME , TMP1 , TMP2 , LNK1 78
C      3      T2M , U , VPR , W , X , Z , LNK1 79
C      4      WHY(40), NDSTR , IDISTR , SPAR1 , SPAR2 , SPAR3 , LNK1 80
C      5      SPAR4 , RMIN , SPAR6 , SPAR7 , SPAR8 , SPAR9 , LNK1 81
C              LNK1 82
C      **** ***** LNK1 83
C              LNK1 84
C      1      FORMAT(12A6) LNK1 85
C      2      FORMAT(1/3X,60HTHE SPECIFIED STANDARD DEVIATION IS NEGATIVE HENCE ILNK1 86
C      INCORRECT///) LNK1 87
C      3      FORMAT(5F10.3) LNK1 88
C      4      FORMAT(1/25X28H**** INPUT PARAMETERS ****/20X,5HYIELD,40X,E12.5LNK1 89
C      1,2X,2HKT/20X,24HHEIGHT OR DEPTH OF BURST,21X,E12.5,2X,6HMETERS/20XLNK1 90
C      2,13H50IL CATEGORY) LNK1 91
C      5      FORMAT(1H+,65X,9HSILICEOUS) LNK1 92
C      6      FORMAT(1H+,65X,10HCALCAREOUS) LNK1 93
C      7      FORMAT(1/20X50HPRE-SHOT SOIL PARTICLE SIZE FREQUENCY DISTRIBUTION/LNK1 94
C      125X32HA LOG-NORMAL DISTRIBUTION WITH -/30X,4HMEAN,31X,E12.5,2X,7HMLNK1 95
C      2ICRONS/30X,18HSTANDARD DEVIATION,17X,E12.5 /25X,34HTHISLNK1 96
C      35 DISTRIBUTION WAS SPECIFIED BY) LNK1 97
C      8      FORMAT(1H+,65X,11HTHE PROGRAM) LNK1 98
C      9      FORMAT(1H+,65X,8HTHE USER) LNK1 99
C      10     FORMAT(15) LNK1 100
C      11     FORMAT(1/3X,58HTHE SCALED DEPTH OF BURST IS BEYOND THE SCOPE OF THELNK1 101
C      1 MODEL///) LNK1 102
C      12     FORMAT(1/3X,11HTHE SCALED HEIGHT OF BURST IS SUCH THAT THERE IS NOLNK1 103
C      1 SOIL MASS ENTRAINED IN THE CLOUD AND HENCE NO LOCAL FALLOUT///) LNK1 104
C      13     FORMAT(1/25X37H**** INITIAL CLOUD PROPERTIES AT H +E12.5,14H SECLNK1 105
C      10NDS ****/20X,23HAVERAGE GAS TEMPERATURE30X,E12.5,2X,14HDEGREES LNK1 106
C      2KELVIN//20X,56HAVERAGE TEMPERATURE OF CONDENSED PHASE MATERIAL IN LNK1 107
C      3CLOUD,5X,E12.5,2X,14HDEGREES KELVIN//20X,31HMASS OF VAPORIZED SOILLNK1 108
C      4 IN CLOUD,30X,E12.5,2X,9HKILOGRAMS//20X,41HMASS OF CONDENSED PHASE LNK1 109
C      5MATERIAL IN CLOUD,20X,E12.5,2X,9HKILOGRAMS//20X,84HPARTICLE SIZE FLNK1 110
C      6FREQUENCY DISTRIBUTION AT THE TIME OF INITIAL CONDITIONS SPECIFICATLNK1 111
C      7ION) LNK1 112
C      14     FORMAT(1H1///51X,14H**** DATA SET 12,6H ****///) LNK1 113
C      15     FORMAT(1X,14HLEAVING LINK 1) LNK1 114
C      16     FORMAT(1H1///51X19H* * * * * //12X101HT HE DEPARTLNK1 115
C      1 MENT OF DEFENSE FALLOUT PREDICT I LNK1 116
C      2 N SYSTEM,///51X,19H* * * * * //43X,36HINITIAL COLNK1 117
C      3NDITIONS (FIREBALL) MODULE///55X,11HPREPARED BY/43X,34HTECHNICAL LNK1 118
C      119

```

```

OPERATIONS RESEARCH, INC./52X, 17H BURLINGTON, MASS.////25X, 45H**** LNK1 120
INITIAL CONDITIONS IDENTIFICATION ****/25X, 12A6) LNK1 121
17 FORMAT(3X, 60H THE SPECIFIED MEAN PARTICLE SIZE IS NEGATIVE HENCE LNK1 122
INCORRECT////) LNK1 123
18 FORMAT(//20X 50H PRE-SHOT SOIL PARTICLE SIZE FREQUENCY DISTRIBUTION/LNK1 124
125X 41H A TABULATED EMPIRICAL DISTRIBUTION WITH -/30X 12, 2X, 21H PARTICL LNK1 125
2LE SIZE CLASSES/30X, 25H MINIMUM PARTICLE DIAMETER, 10X, E12.5, 2X, 7H MIC LNK1 126
3CRONS/25X, 43H THIS DISTRIBUTION WAS SPECIFIED BY THE USER) LNK1 127
19 FORMAT(25X, 37H THE DISTRIBUTION IS LOG-NORMAL WITH -/30X, 4H MEAN, 31X LNK1 128
1, E12.5, 2X, 7H MICRONS/30X, 18H STANDARD DEVIATION, 17X, E12.5 LNK1 129
2 /30X, 25H MINIMUM PARTICLE DIAMETER, 10X, E12.5, 2X, 7H MICRONS) LNK1 130
191 FORMAT(25X, 48H THE DISTRIBUTION IS THE SAME AS THAT GIVEN ABOVE) LNK1 131
192 FORMAT(//51X, 19H * * * * * //) LNK1 132
193 FORMAT(//31X, 19H PARTICLE SIZE CLASS, 20X, 13H MASS FRACTION/) LNK1 133
194 FORMAT(40X, 12, 29X, E12.5) LNK1 134
C ***** LNK1 135
C ***** LNK1 136
C ***** LNK1 137
C NM=1 LNK1 138
C READ INITIAL CONDITIONS RUN IDENTIFIER LNK1 139
READ (ISIN, 1) (DETID(J), J=1, 12) LNK1 140
C READ CONTROL INTEGER LNK1 141
READ (ISIN, 10) N LNK1 142
C LNK1 143
C WRITE OVERALL TITLE LNK1 144
WRITE (ISOUT, 16) (DETID(J), J=1, 12) LNK1 145
20 READ (ISIN, 10) IDISTR LNK1 146
IF (IDISTR) 210, 210, 211 LNK1 147
C 210 TEST FOR PARTICLE SIZE FREQUENCY SPECIFICATION OPTION LNK1 148
210 READ (ISIN, 3) W, X, U, DIAM, SD LNK1 149
READ (ISIN, 3) DMIN LNK1 150
RMIN=0.5*DMIN LNK1 151
C WAS A PRESLOT PARTICLE LOG-NORMAL DISTRIBUTION SPECIFIED BY LNK1 152
C THE USER YES TO 22 LNK1 153
IF (DIAM) 21, 21, 22 LNK1 154
21 IS=0 LNK1 155
GO TO 23 LNK1 156
22 IS=1 LNK1 157
GO TO 23 LNK1 158
211 READ (ISIN, 3) W, X, U LNK1 159
READ (ISIN, 3) DMIN LNK1 160
RMIN=0.5*DMIN LNK1 161
READ (ISIN, 10) NDSTR LNK1 162
READ (ISIN, 3) (WHY(I), I=1, NDSTR) LNK1 163
C LNK1 164
C 23 CONVERT HOB - DOB FROM METERS TO FEET LNK1 165
23 X=X/0.3048 LNK1 166
C Z IS THE SCALED HOB - DOB LNK1 167
60 Z=X/((W)**(1.0/3.4)) LNK1 168
C LNK1 169
C TEST THE DATA TO SEE IF THE MODEL IS APPROPRIATE LNK1 170
IF (X) 66, 63, 63 LNK1 171
63 IF (Z-180.0) 70, 70, 150 LNK1 172
66 IF (Z+20.0) 143, 70, 70 LNK1 173
70 CALL TIME LNK1 174
CALL TEMP LNK1 175
CALL MASS LNK1 176
CALL VAPOR LNK1 177
IF (IDISTR) 90, 90, 96 LNK1 178
LNK1 179

```

CALL TEMP	LNK1 180
CALL MASS	LNK1 181
CALL VAPOR	LNK1 182
IF(IDISTR)90,90,96	LNK1 183
C	LNK1 184
C TEST FOR ACCEPTABLE SPECIFICATIONS OF PRE-SHOT PARTICLE SIZE	LNK1 185
C FREQUENCY DISTRIBUTION.	LNK1 186
90 IF(SD)91,92,92	LNK1 187
91 WRITE (ISOUT,2)	LNK1 188
GO TO 93	LNK1 189
92 IF(DIAM)94,95,96	LNK1 190
94 WRITE (ISOUT,17)	LNK1 191
C 93 SHOULD THE RUN BE HALTED. YES TO 190	LNK1 192
93 IF(N)190,190,170	LNK1 193
C	LNK1 194
95 CALL DSTBN	LNK1 195
C	LNK1 196
C CONVERT HOB - DOB BACK TO METERS FROM FEET	LNK1 197
96 X=X*0.3048	LNK1 198
C	LNK1 199
C CONVERT VPR AND SSAM FROM GRAMS TO KILOGRAMS	LNK1 200
VPR=VPR/1000.0	LNK1 201
C DURING COMPUTATION SSAM CONTAINS THE VALUE OF THE TOTAL MASS OF	LNK1 202
C GAS AND CONDENSED PHASE MATERIAL IN THE CLOUD.	LNK1 203
SSAM=SSAM/1000.0-VPR	LNK1 204
C	LNK1 205
C WRITE INITIAL CONDITIONS RESULTS	LNK1 206
WRITE (ISOUT,4)W,X	LNK1 207
IF(U-1.0)301,301,302	LNK1 208
301 WRITE (ISOUT,5)	LNK1 209
GO TO 305	LNK1 210
302 WRITE (ISOUT,6)	LNK1 211
305 IF(IDISTR)310,310,311	LNK1 212
310 WRITE(ISOUT,7)DIAM,SD	LNK1 213
IF (IS)102,103,102	LNK1 214
311 WRITE(ISOUT,18)NDSTR,DMIN	LNK1 215
WRITE(ISOUT,193)	LNK1 216
WRITE(ISOUT,194;(:,WHY(I),I=1,NDSTR)	LNK1 217
GO TO 106	LNK1 218
103 WRITE (ISOUT,8)	LNK1 219
GO TO 106	LNK1 220
102 WRITE (ISOUT,5)	LNK1 221
106 WRITE(ISOUT,13)TME,TMP1,TMP2,VPR,SSAM	LNK1 222
IF(IDISTR)116,116,117	LNK1 223
116 WRITE(ISOUT,19)DIAM,SD,DMIN	LNK1 224
GO TO 118	LNK1 225
117 WRITE(ISOUT,191)	LNK1 226
118 WRITE(ISOUT,192)	LNK1 227
GO TO 171	LNK1 228
143 WRITE (ISOUT,11)	LNK1 229
GO TO 171	LNK1 230
150 WRITE (ISOUT,12)	LNK1 231
C	LNK1 232
C TEST TO DETERMINE WHETHER TO CALL LINK 2, RETURN TO COMPUTE	LNK1 233
C ANOTHER SET OF INITIAL CONDITIONS, OR EXIT.	LNK1 234
171 IF(N-1)200,200,170	LNK1 235
170 IF(N-NN)190,190,180	LNK1 236
180 NN=NN+1	LNK1 237
WRITE (ISOUT,14)NN	LNK1 238
GO TO 20	LNK1 239

200 WRITE (ISOUT,15)
RETURN
190 STOP
END

LNK1 240
LNK1 241
LNK1 242
LNK1 243

SIBFTC	DSTB	LIST,DECK,M94/2	DSTB	0
		SUBROUTINE DSTBN	DSTB	1
C			DSTB	2
C	*****		DSTB	3
C			DSTB	4
	COMMON /SET1/		DSTB	5
1	DIAM	, FID , IRISE , IEXEC , ISIN , ISZUT ,	DSTB	6
2	SD	, SPAR , SSAM , TME , TMP1 , TMP2 ,	DSTB	7
3	T2H	, U , VPR , W , X , Z ,	DSTB	8
4	WHY	, NDSTR , IDISTR , SPAR1 , SPAR2 , SPAR3 ,	DSTB	9
5	SPAR4	, RMIN , SPAR6 , SPAR7 , SPAR8 , SPAR9	DSTB	10
	DIMENSION FID(12)		DSTB	11
	DIMENSION WHY(40)		DSTB	12
C			DSTB	13
C	*****		DSTB	14
C	*****		DSTB	15
C			DSTB	16
	DIAM=0.407		DSTB	17
	SD=4.00		DSTB	18
	RETURN		DSTB	19
	END		DSTB	20

SIBFTC MAS	LIST,DECK,M94/2	MAS	0
	SUBROUTINE MASS	MAS	1
C		MAS	2
C	*****	MAS	3
C		MAS	4
	COMMON /SET1/	MAS	5
1	DIAM , FID , IRISE , IEXEC , ISIN , ISOUT ,	MAS	6
2	SD , SPAR , SSAM , TME , TMP1 , TMP2 ,	MAS	7
3	T2M , U , VPR , W , X , Z ,	MAS	8
4	WHY , NDSTR , IDISTR , SPAR1 , SPAR2 , SPAR3 ,	MAS	9
5	SPAR4 , RM'N , SPAR6 , SPAR7 , SPAR8 , SPAR9	MAS	10
	DIMENSION FID(12)	MAS	11
	DIMENSION WHY(40)	MAS	12
C		MAS	13
C	*****	MAS	14
C	*****	MAS	15
C		MAS	16
	H08 OR D08	MAS	17
	IF(X)230,240,240	MAS	18
230	D=2181.595	MAS	19
	Q=-Z	MAS	20
	R=1.125E+02+(7.55E-01)*Q-(9.6E-06)*(Q**3.0)-(9.11E-12)*(Q**5.0)	MAS	21
	S=3.27E+01+(8.51E-01)*Q-(2.52E-05)*(Q**3.0)+(1.78E-10)*(Q**5.0)	MAS	22
	SSAM= D*((W)**(3.0/3.4))*(R**2.0)*S	MAS	23
	GO TO 250	MAS	24
240	E=77.40685	MAS	25
	SSAM= E*((W)**(3.0/3.4))*((180.0-Z)**2.0)*(360.0+Z)	MAS	26
250	RETURN	MAS	27
	END	MAS	28

SIBFTC TEM	LIST,DECK,M94/2	TEM	0
SUBROUTINE TEMP		TEM	1
C		TEM	2
C	*****	TEM	3
C		TEM	4
	COMMON /SET1/	TEM	5
1	D*AM , FID , IRISE , IEXEC , IS, / , ISOUT ,	TEM	6
2	SD , SPAR , SSAM , TME , TMP1 , TMP2 ,	TEM	7
3	T2M , U , VPR , U , X , Z ,	TEM	8
4	WHY , NDSTR , IDISTR , SPAR1 , SPAR2 , SPAR3 ,	TEM	9
5	SPAR4 , RMIN , SPAR6 , SPAR7 , SPAR8 , SPAR9	TEM	10
	DIMENSION FID(12)	TEM	11
	DIMENSION WHY(40)	TEM	12
C		TEM	13
C	*****	TEM	14
C	*****	TEM	15
C		TEM	16
C	COMPUTE VAPOR TEMPERATURE	TEM	17
	Q=Z*W**(-.03921)	TEM	18
	A=5980.*((1.145)**(Q/180.))*(W)**(-0.03948+0.02637*Q/180.0)	TEM	19
	B=-0.4473*(W**(0.04360))	TEM	20
	TMP1=A*((TME/T2M)**B)+1500.0	TEM	21
C		TEM	22
C	COMPUTE CONDENSED PHASE MATERIAL TEMPERATURE	TEM	23
	TMP2=50.0*ALOG10(W)+1400.0	TEM	24
	RETURN	TEM	25
	END	TEM	26

SIBFTC	TIM	LIST,DECK,M94/2	TIM	0
		SUBROUTINE TIME	TIM	1
C			TIM	2
C		*****	TIM	3
C			TIM	4
		COMMON /SET1/	TIM	5
1		DIAM , FID , IRISE , IEXEC , ISIN , ISOUT ,	TIM	6
2		SD , SPAR , SSAM , TME , TMP1 , TMP2 ,	TIM	7
3		TZA , U , VPR , W , X , Z ,	TIM	8
4		WHY , NDSTR , IDISTR , SPAR1 , SPAR2 , SPAR3 ,	TIM	9
5		SPAR4 , RMIN , SPAR6 , SPAR7 , SPAR8 , SPAR9	TIM	10
		DIMENSION FID(12)	TIM	11
		DIMENSION WHY(40)	TIM	12
C			TIM	13
C		*****	TIM	14
C		*****	TIM	15
C			TIM	16
		Q=Z*W**(-.03921)	TIM	17
		T2M=0.037*((0.045/0.037)**(Q/180.))*(W**(0.49-(0.07*Q/180.)))	TIM	18
		TME=(56.0*T2M)/(W**(0.3))	TIM	19
		RETURN	TIM	20
		END	TIM	21

SIBFTC VAP0	LIST,DECK,M94/2	VAP0	0
	SUBROUTINE VAP0R	VAP0	1
C		VAP0	2
C	*****	VAP0	3
C		VAP0	4
	COMMON /SET1/	VAP0	5
1	DIAM , FID , IRISE , IEXEC , ISIN , ISOUT ,	VAP0	6
2	SJ , SPAR , SSAM , TME , TMP1 , TMP2 ,	VAP0	7
3	T2M , U , VPR , W , X , Z ,	VAP0	8
4	WHY , NDSTR , IDISTR , SPAR1 , SPAR2 , SPAR3 ,	VAP0	9
5	SPAR4 , RMIN , SPAR6 , SPAR7 , SPAR8 , SPAR9	VAP0	10
	DIMENSION FID(12)	VAP0	11
	DIMENSION WHY(40)	VAP0	12
C		VAP0	13
C	*****	VAP0	14
C	*****	VAP0	15
C		VAP0	16
C	BRANCH ON THE BASIS OF SOIL CATEGORY -SILICEOUS TO 100,	VAP0	17
C	CALCAPEOUS TO 200	VAP0	18
	IF(U-1.0)100,100,200	VAP0	19
C		VAP0	20
C	IS THE COMPUTED VAPOR TEMPERATURE HIGHER THAN THE SILICEOUS SOIL	VAP0	21
C	BOILING TEMPERATURE	VAP0	22
100	IF(TMP1-3000.0)120,120,110	VAP0	23
110	VPR=SSAM*0.00015*(TMP1-3000.0)	VAP0	24
	GO TO 130	VAP0	25
C		VAP0	26
C	IS THE COMPUTED VAPOR TEMPERATURE HIGHER THAN THE CALCAPEOUS SOIL	VAP0	27
C	BOILING TEMPERATURE	VAP0	28
200	IF(TMP1-3100.0)120,120,115	VAP0	29
115	VPR=SSAM*0.00015*(TMP1-3100.0)	VAP0	30
	GO TO 130	VAP0	31
120	VPR=0.0	VAP0	32
130	RETURN	VAP0	33
	END	VAP0	34

 THE DEPARTMENT OF DEFENSE FALLOUT PREDICTION SYSTEM

INITIAL CONDITIONS (FIREBALL) MODULE

PREPARED BY
 TECHNICAL OPERATIONS RESEARCH, INC.
 BURLINGTON, MASS.

*** INITIAL CONDITIONS IDENTIFICATION ***
 DEBUG TEST OF INITIAL CONDITIONS MODEL

*** INPUT PARAMETERS ***

YIELD +0.10000E+01 KT
 HEIGHT OR DEPTH OF BURN +0.00000E-30 MET RS
 SOIL CATEGORY SILICEOUS

PRE-SHOT SOIL PARTICLE SIZE FREQUENCY DISTRIBUTION

A LOG-NORMAL DISTRIBUTION WITH
 MEAN +0.65290E+01 MICRONS
 STANDARD DEVIATION +0.39660E+01
 THIS DISTRIBUTION WAS SPECIFIED BY THE PROGRAM

*** INITIAL CLOUD PROPERTIES AT H +0.20720E+01 SECONDS ***

AVERAGE GAS TEMPERATURE +0.24880E+04 DEGREES KELVIN
 AVERAGE TEMPERATURE OF CONDENSED PHASE MATERIAL IN CLOUD +0.14000E+04 DEGREES KELVIN
 MASS OF VAPORIZED SOIL IN CLOUD +0.00000E-30 KILOGRAMS
 MASS OF CONDENSED PHASE MATERIAL IN CLOUD +0.90287E+06 KILOGRAMS

PARTICLE SIZE FREQUENCY DISTRIBUTION AT THE TIME OF INITIAL CONDITIONS SPECIFICATION
 THE DISTRIBUTION IS LOG-NORMAL WITH

MEAN +0.65290E+01 MICRONS
 STANDARD DEVIATION +0.39660E+01
 MINIMUM PARTICLE DIAMETER

LEAVING LINK 1
 ENTERING LINK 2

THE DEPARTMENT OF DEFENSE FALLOUT PREDICTION SYSTEM

INITIAL CONDITIONS (FIREBALL) MODULE

PREPARED BY
TECHNICAL OPERATIONS RESEARCH, INC.
BURLINGTON, MASS.

**** INITIAL CONDITIONS IDENTIFICATION ****
DENDU TEST OF INITIAL CONDITIONS MODEL

**** INPUT PARAMETERS ****

YIELD +0.10000E+01 KT
HEIGHT OR DEPTH OF BURST +0.00000E+30 METERS
SOIL CATEGORY SILICEOUS

PRE-SHOT SOIL PARTICLE SIZE FREQUENCY DISTRIBUTION
A TABULATED EMPIRICAL DISTRIBUTION WITH
40 PARTICLE SIZE CLASSES
MINIMUM PARTICLE DIAMETER +0.10000E+02 MICRONS
THIS DISTRIBUTION WAS SPECIFIED BY THE USER

PARTICLE SIZE CLASS	MASS FRACTION
1	+0.25000E-01
2	+0.25000E-01
3	+0.25000E-01
4	+0.25000E-01
5	+0.25000E-01
6	+0.25000E-01
7	+0.25000E-01
8	+0.25000E-01
9	+0.25000E-01
10	+0.25000E-01
11	+0.25000E-01
12	+0.25000E-01
13	+0.25000E-01
14	+0.25000E-01
15	+0.25000E-01
16	+0.25000E-01
17	+0.25000E-01
18	+0.25000E-01
19	+0.25000E-01
20	+0.25000E-01
21	+0.25000E-01
22	+0.25000E-01
23	+0.25000E-01
24	+0.25000E-01
25	+0.25000E-01
26	+0.25000E-01
27	+0.25000E-01
28	+0.25000E-01
29	+0.25000E-01
30	+0.25000E-01
31	+0.25000E-01
32	+0.25000E-01
33	+0.25000E-01
34	+0.25000E-01
35	+0.25000E-01
36	+0.25000E-01
37	+0.25000E-01
38	+0.25000E-01
39	+0.25000E-01
40	+0.25000E-01

**** INITIAL CLOUD PROPERTIES AT H +0.20720E+01 SECONDS ****

AVERAGE GAS TEMPERATURE +0.24887E+04 DEGREES KELVIN
AVERAGE TEMPERATURE OF CONDENSED PHASE MATERIAL IN CLOUD +0.14000E+04 DEGREES KELVIN
MASS OF VAPORIZED SOIL IN CLOUD +0.00000E+30 KILOGRAMS
MASS OF CONDENSED PHASE MATERIAL IN CLOUD +0.90287E+06 KILOGRAMS
PARTICLE SIZE FREQUENCY DISTRIBUTION AT THE TIME OF INITIAL CONDITIONS SPECIFICATION
THE DISTRIBUTION IS THE SAME AS THAT GIVEN ABOVE

LEAVING LINK 1
ENTERING LINK 2

REFERENCES

1. I. O. Huebsch, "The Development of a Water-Surface-Burst Fallout Model: The Rise and Expansion of the Atomic Cloud," USNRDL-TR-741 (23 April 1964).
2. I. O. Huebsch, "Development of a Land Surface Burst Cloud Rise Model," USNRDL-LR-145 (1965). (To be superseded by a USNRDL-TR)
3. H. G. Norment, W. Y. G. Ing, and J. Zuckermen, "Initial Conditions in the Nuclear Cloud," Technical Operations Research, Burlington, Mass., TO-B 65-118, AD369604 (February 1966). Secret-F. R. D.
4. H. G. Norment and S. Woolf, "Studies of Nuclear Cloud Rise and Growth Data," Proceedings of the Joint DASA-OCD Fallout Symposium, Monterey, California (12-14 April 1966). Secret-F. R. D.
5. H. G. Norment and S. Woolf, "Studies of Nuclear Cloud Rise and Growth," Technical Operations Research, Burlington, Mass., TO-B 66-9 (to be published). Secret-F. R. D.
6. Unpublished document on Cloud Characteristics, Edgeron, Germeshausen and Grier Report No. ET-833, prepared on contract AT(29-1) 1183. Secret-F. R. D.
7. R. W. Hillendahl, "Characteristics of the Thermal Radiation from Nuclear Detonations (U)," Vol. III, Naval Radiological Defense Laboratory, NRDL-TR-383 (30 June 1959). Secret-RD.
8. M. D. Nordyke, "On Cratering: A Brief History, Analysis, and Theory of Cratering," Lawrence Radiation Laboratory, UCRL-6578 (22 August 1961).
9. R. L. Stetson et al., "Distribution and Intensity of Fallout from the Underground Shot," Operation TEAPOT - Project 2.5.2, Naval Radiological Defense Laboratory, WT-1154 (14 March 1958).
10. P. D. LaRiviere et al., "Fallout Collection and Gross Sample Analysis (U)," Operation SUN BEAM, Shot Small Poy, Project 2.9, Naval Radiological Defense Laboratory, POR-2215 (October 1964). Secret-RD.

11. M. Morgenthau et al., "Compilation of Fallout Patterns and Test Data. Vol. II. Local Fallout from Nuclear Test Detonations," Nuclear Defense Laboratory, NDL-TR-34, DASA 1251 (August 1963). Secret-RD.
12. R. M. Davies and G. I. Taylor, "The Mechanics of Large Bubbles Rising Through Extended Liquids and Through Liquids in Tubes," Proc. Roy. Soc. A200, 375 (1950).
13. G. K. Batchelor, "Heat Convection and Buoyancy Effects in Fluids," Quarterly J. Roy. Meteor. Soc. 80, 339 (1954).
14. S. Glasstone, editor, "The Effects of Nuclear Weapons" (Washington, D. C. : USAEC, 1962).
15. H. G. Norment, "Research on Circulation in Nuclear Clouds," Technical Operations, Incorporated, TO-B 63-102 (1 December 1963).
16. H. G. Norment, "Research on Circulation in Nuclear Clouds, II (U)," Technical Operations, Incorporated, TO-B 64-102 (1 November 1964). Confidential-F. R. D.
17. J. F. Moulton, Jr., "Nuclear Weapons Blast Phenomena," U.S. Naval Ordnance Laboratory, DASA-1200 (March 1960). Section 1.5. Secret-RD.
18. B. Alder, S. Fernbach, and M. Rolenbert, editors, Methods in Computational Physics, Vol. 3, Fundamental Methods in Hydrodynamics (New York, N. Y. : Academic Press, 1964).
19. K. Stewart, "The Condensation of a Vapor to an Assembly of Droplets of Particles (with Particular Reference to Atomic Explosion Debris)," Trans. Fara. Soc. 52, 161 (1956).
20. M. Morgenthau et al., "Land Fallout Studies (U)," Operation REDWING - Project 2.65, Chemical Warfare Laboratories, WT-1319 (1 February 1960). Secret-RD.
21. C. F. Miller, "Fallout and Radiological Countermeasures," Vol. I, Stanford Research Institute, SRI Project No. IM-4021 (January 1963). Chapter 3.
22. R. D. Cadle, "The Effects of Soil, Yield, and Scaled Depth on Contamination from Atomic Bombs," Stanford Research Institute, Project No. Cu-640 (29 June 1953). Secret-RD.

23. R. G. Gutmacher and G. H. Higgins, "Total Mass and Concentration of Particles in Dust Clouds (U)," UCRL-14397 (28 September 1965). Secret-RD.
24. B. Mason, "Principles of Geochemistry" (New York, N. Y. : John Wiley & Sons, 1952), p. 38ff.
25. H. L. Shick, "A Thermodynamic Analysis of the High Temperature Vaporization Properties of Silica," *Cnem. Rev.* 60, 331 (1960).
26. C. D. Hodgman, editor, "Handbook of Chemistry and Physics," 44th Edition, The Chemical Rubber Publishing Co., Cleveland (1962).
27. E. C. Fretling, L. R. Bunney, and F. K. Kawahara, "Physico-chemical and Radiochemical Analysis (U)," Operation SUN BEAM, Shot Small Boy, Project 2.10, POR-2216, Naval Radiological Defense Laboratory (15 October 1964).
28. D. E. Clark, F. K. Kawahara, and W. C. Cobbin, "Fallout Sampling and Analysis: Radiation Dose Rate and History at 16 Locations (U)," Operation SUN BEAM, Shot Johnie Boy, Project 2.9, POR-2289, Naval Radiological Defense Laboratory (12 October 1963). Secret-RD.
29. "Capabilities of Atomic Weapons," Department of the Army Technical Manual, TM 23-200 (June 1955). Secret-RD.

APPENDIX A

FORM OF THE TEMPERATURE EQUATION

Let us visualize a rising nuclear cloud as a turbulent eddy of hot air that is being cooled by the mixing in of entrained ambient air. The effect of mixing on the average cloud temperature can be estimated from a calorimeter equation: if ΔT is the temperature change due to the entrainment of mass ΔM ,

$$MTC_p + \Delta MT_o C_p = (M + \Delta M)(T + \Delta T) C_p,$$

where M and T are cloud mass and temperature prior to the entrainment of mass ΔM , T_o is the ambient temperature, and C_p is heat capacity. This gives

$$\frac{dT}{dt} = - (T - T_o) \frac{1}{M} \frac{dM}{dt}.$$

The quantity $(1/M)(dM/dt)$ can be interpreted as being proportional to the reciprocal of a mixing time, τ , so we may write

$$-\frac{dT}{dt} \propto (T - T_o) \frac{1}{\tau}. \quad (A.1)$$

A characteristic scale length for the cloud will be the radius R , and a characteristic eddy velocity will be of the order of the cloud-rise velocity v . The effective turbulent diffusion "constant" would then be of the order of $D = Rv$. From well-known solutions to the diffusion equation, we then infer that a typical mixing time τ will be of the order $R^2/D = R/v$, a not unexpected result. Equation (A.1) becomes

$$-\frac{dT}{dt} \propto \frac{v}{R} (T - T_o). \quad (A.2)$$

The essence of this derivation has been presented in Ref. A.1.

Our study of cloud-rise data obtained from movie films of nuclear test shots^{A.2} has led to the relations

$$R \propto z \quad (A.3)^*$$

and

$$v \propto \frac{z}{t}, \quad (A.4)$$

where z is cloud center altitude.

Substituting Eqs. (A.3) and (A.4) into Eq. (A.2), we obtain

$$\frac{dT}{dt} = n \frac{T - T_o}{t} \quad (A.5)$$

Upon integration of Eq. (A.5), using conditions at the second temperature maximum at the lower limits, we have

$$T - T_o = (T_{2m} - T_o) \left(\frac{t}{t_{2m}} \right)^n$$

The factor $T_{2m} - T_o$ is almost a constant that we shall represent by K , and we arrive at the equation

$$T = K \left(\frac{t}{t_{2m}} \right)^n + T_o \quad (A.6)$$

In using Eq. (A.6), we should not forget that it is based on crude analogies and loose dimensional analyses. Its major virtue is that it fits the form of the observed data. Accordingly, we should not be surprised if certain of the equation parameters turn out to have values different from those that we would expect on the basis of their literal interpretations as implied in the equation derivation.

* Equation (A.3) also has been observed from experiments in water tanks^{A.3-A.5} and has been derived by Taylor^{A.6} and Batchelor.^{A.7}

REFERENCES

- A. 1 "Study of Optical and Infrared Whiteout by Nuclear Detonations (U), " Technical Operations Research, TO-B 63-57, Prepared for AVCO Corp. , Wilmington, Mass. under subcontract number 107682 (30 June 1963). Secret-RD.
- A. 2 Unpublished Document on Cloud Characteristics, Edgerton, Germeshausen and Grier Report No. ET-383, prepared on contract AT(29-1)1183. Secret-FRD.
- A. 3 B. R. Morton, G. I. Taylor, and J. S. Turner, "Turbulent Convection from Maintained and Instantaneous Sources, " Proc. Roy. Soc. (London) A. 234, 1 (1956).
- A. 4 R. S. Scorer, "Experiments on Convection of Isolated Masses of Buoyant Fluid, " J. Fluid Mech. 2, 583 (1957).
- A. 5 J. S. Turner, "Buoyant Vortex Rings, " Proc. Roy. Soc. (London) 239A, 61 (1957).
- A. 6 G. I. Taylor, "Dynamics of a Mass of Hot Gas Rising in Air, " USAEC MDDC-919 (16 March 1945).
- A. 7 G. K. Batchelor, "Heat Convection and Buoyancy Effects in Fluids, " Quart. J. Roy. Met. Soc. 80, 339 (1954).

APPENDIX B

CHARACTERIZATION OF THE UNVAPORIZED PORTION OF THE CLOUD SOIL BURDEN

In this appendix we describe the results of simple energy conservation calculations for nuclear detonations that are designed to yield information on the relation of the temperature of unvaporized soil at t_i , the time of initial conditions specification, to the combined influences of detonation energy yield, fraction of this energy remaining in the cloud at t_i , height of burst, and the fraction of the soil burden vaporized. An example is presented of how this information can be used to obtain estimates of the fraction of the soil burden vaporized and the average temperature of the unvaporized portion of the soil burden.

Energy Conservation Calculations

Our energy conservation calculations are based in part on the following assumptions:

1. Each kiloton of detonation energy yield is equivalent to 4.2×10^{12} J (Ref. B.1, Table 1.41).
2. The average temperature of the gaseous contents of the cloud at t_i is given by Eqs. (6), (7), and (8) of this volume.
3. The gaseous contents of the cloud obeys the ideal gas equation of state.
4. The total mass of the soil burden is given by Eq. (10) or Eq. (15).

Also of critical importance are: specific heats c_a (J/(deg-kg)) for air (Ref. B.2), where

$$c_a = \begin{cases} 946.6 + 0.1971T, & T < 2300^\circ\text{K} \\ -3587.5 + 2.125T, & T \geq 2300^\circ\text{K} \end{cases}, \quad (\text{B.1})$$

and for soil (quartz) (Ref. B. 3), c_s , where*

$$c_s = \begin{cases} 781.6 + 0.5712T - \frac{1.881 \times 10^7}{T^2}, & T < 848^\circ\text{K} \\ 1003.8 + 0.1351T, & T \geq 848^\circ\text{K} \end{cases} \quad (\text{B. 2})$$

the heat of vaporization per kilogram of soil (SiO_2) (Ref. B. 4), Δh_v , where

$$\Delta h_v = 1.0313 \times 10^7 - 482.3T \quad ; \quad \dagger \quad (\text{B. 3})$$

and cloud volume, $V = \frac{4}{3}\pi R^2 H$, where R and H are respectively the horizontal and vertical cloud radii. These radii have been determined as functions of time and yield from analyses of photographic observations of nuclear test shot clouds (Ref. B. 5). At t_1 , the cloud volume (cubic meters) is given by

$$V = 1.78 \times 10^6 W^{0.928}, \quad (\text{B. 4})$$

where W is the detonation yield in kilotons. The cloud center height, Z , (for surface and airbursts) (meters) at t_1 is given by

$$Z = h + 108W^{0.349},$$

where h is the height of burst in meters. Pressure at the altitude Z is taken as that of the ARDC model atmosphere (Ref. B. 6).

* Calculations were done using the quartz data only. Specific heats for calcium oxide (CaO) are about 20% less than for SiO_2 so that for the high yield Pacific shots we have overestimated the energy required to heat the soil by this amount.

† Heat of fusion energy has not been included in the calculations. According to Coughlin^{B. 8} $\Delta h_f = 1.36 \times 10^5$ J/kg. Compared with the other energy changes considered, this is negligible.

If the vaporized fraction of the total soil burden is specified, then the mass of the air in the cloud, m_a , is given by

$$m_a = M_a \left(\frac{PV}{T_g R} - \frac{m_s^g}{M_s} \right) \quad , \quad (B. 5)$$

where M_a and M_s are the average molecular weights of air and soil respectively, m_s^g is the mass of soil gas, R is the universal gas constant, P is pressure, and T_g is the average temperature of the cloud gases.

If, in addition, the total energy available for heating and vaporizing the cloud contents is known, then the average temperature of unvaporized soil is obtained from the relation,

$$T_c = 293 + \frac{fW - Q_g}{m_s^c c_s} \quad , \quad (B. 6)$$

where T_c is the average temperature of unvaporized material, W is the total detonation energy yield, f is the fraction of the total energy available for heating the cloud contents, m_s^c is the mass of unvaporized soil, and Q_g is the energy (i. e., heat content) of the cloud gases relative to the ambient condition. Q_g is given by

$$Q_g = \left(m_a c_a + m_s^g c_s \right) (T_g - 293) + m_s^g \Delta h_v \quad , \quad (B. 7)$$

where Δh_v is the heat of vaporization of the soil.

Using these relations, detailed calculations were performed for values of f varying stepwise from 0.1 to 0.9, and for values of m_s^g representing fractions of the total soil burden from 0 to 0.2, for the range of yields from 0.01 KT to 100 MT and heights of burst from -20 to 150 scaled feet relative to mean sea level. The restriction that $300 \leq T_c \leq 3000$ was imposed. Needless to say, these calculations were done on a digital computer.

These calculations served to bracket the ranges of conditions within which energy balances can be attained. Illustrative graphs are shown in Figure B.1 (a-e). Values of T_c are given for those points where energy balances can be obtained. Where energy cannot be conserved, a + indicates a surplus of available energy and a - indicates a deficit of available energy. It is apparent from these graphs, that

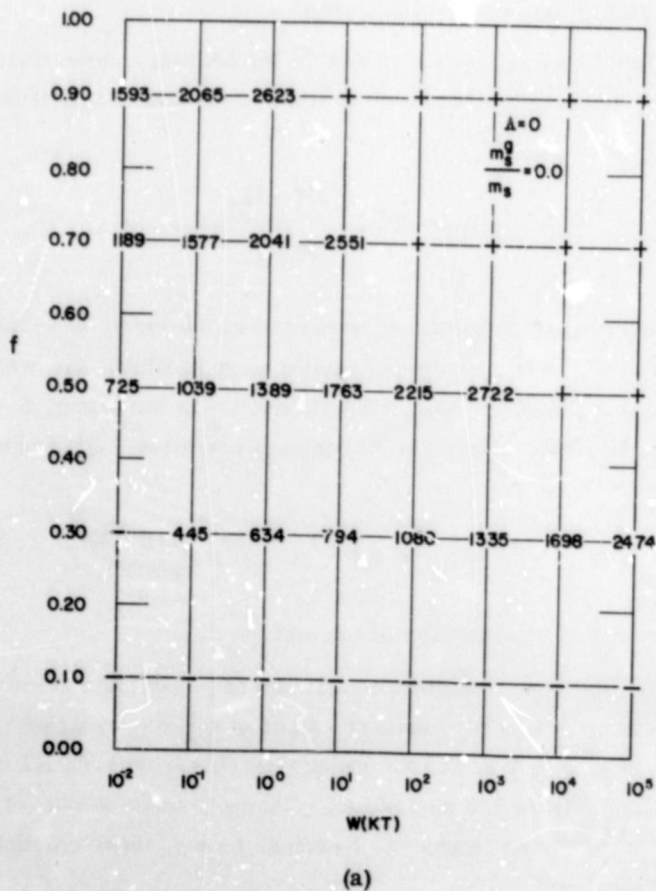
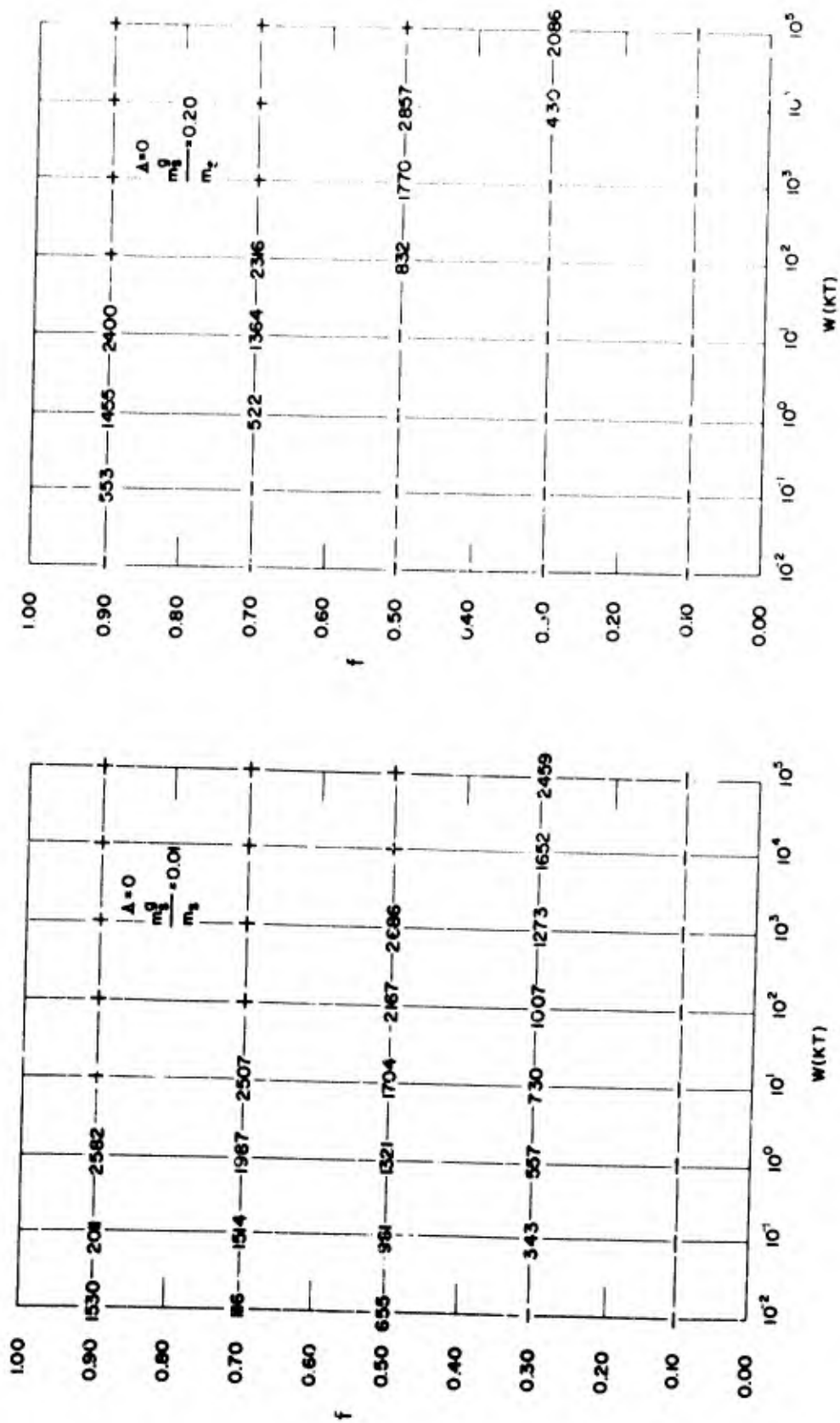


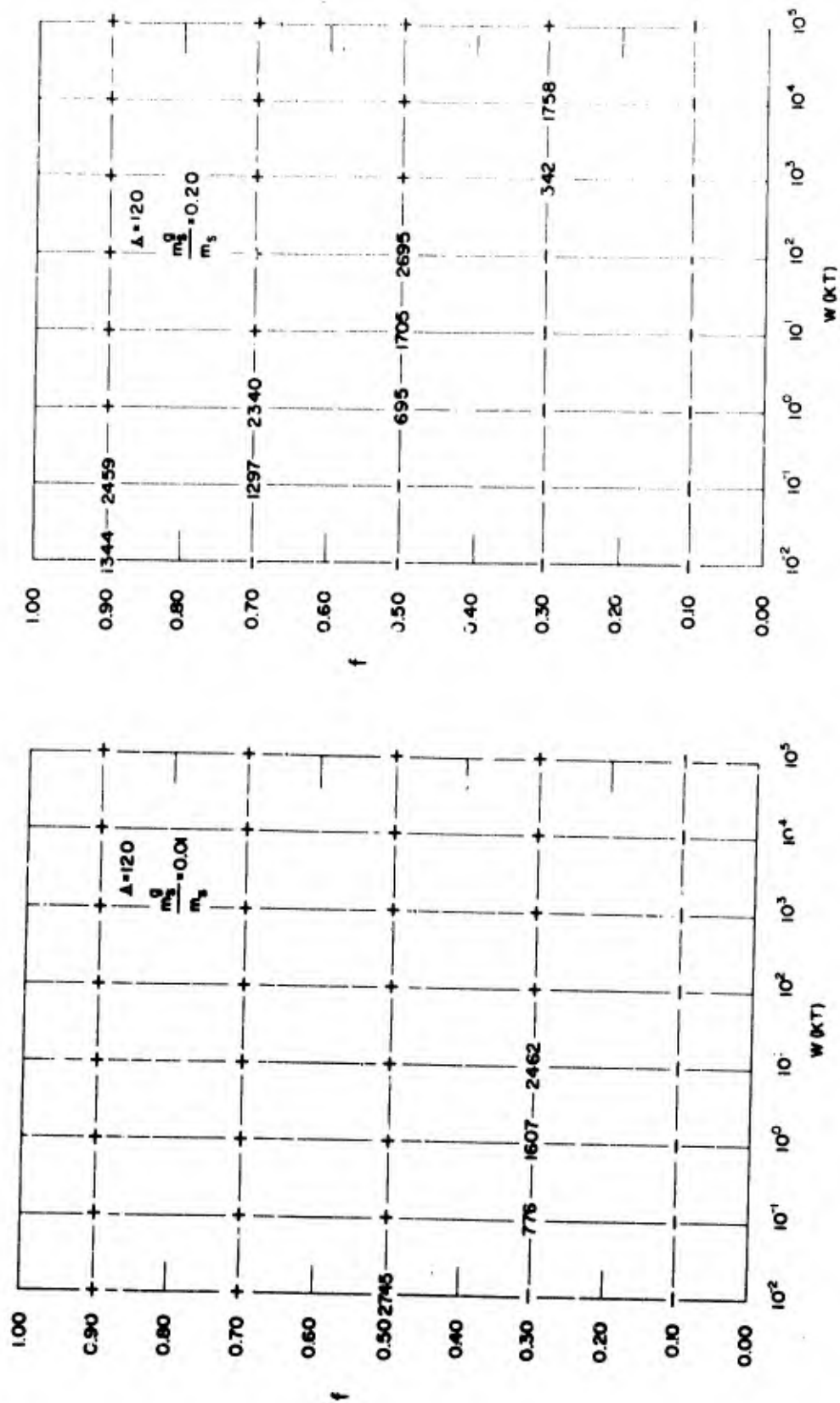
Figure B.1. Illustrative Graphs that Show Relationship Between Yield and Energy Available for Heating for Several Heights of Burst (See text for further explanation.)



(b)

(c)

Figure B.1 (Cont'd.) Illustrative Graphs that Show Relationship Between Yield and Energy Available for Heating for Several Heights of Burst (See text for further explanation.)



(d)

(e)

Figure B.1 (Cont'd.) Illustrative Graphs that Show Relationship Between Yield and Energy Available for Heating for Several Heights of Burst (See text for further explanation.)

a wide range of physically reasonable possibilities exist for values of f and m_s^g . Accordingly, it is mandatory that a means be found to select appropriate values for these parameters for specified yield and height of burst.

An Example Procedure for Specifying f and m_s^g

As noted previously, the central problem in the specification of f and m_s^g is in determining the fraction of the total energy yield available for heating air and soil. In the process of casting about for a reasonable method for determining this energy fraction, we found the following equations in the 1955 edition of the "Capabilities of Atomic Weapons" (Ref. B. 7) for the thermal energy yield Q_T for air and surface bursts:

$$Q_{T,a} = 0.44W^{0.94}, \quad \text{air bursts} \quad , \quad (B. 8)$$

$$Q_{T,s} = 0.147W, \quad \text{surface bursts} \quad . \quad (B. 9)$$

In our example procedure we assume the relations

$$fW = (Q_{T,a} - Q_{T,s}) H \quad (B. 10)$$

and

$$m_s^g > 0 \quad \text{only if} \quad T_g > 3000^\circ . \quad (B. 11)^*$$

H is a factor to account for height of burst that has the forms of the height of burst scaling factors used for the soil burden calculations (Eqs. (10) and (15)):

$$H = \frac{R^2(z)D(z)}{(112.7)^2(32.7)} , \quad \Lambda < 0 ,$$

$$H = \frac{(180 - \Lambda)^2(360 + \Lambda)}{(180)^2(360)} , \quad \Lambda \geq 0 , \quad (B. 12)$$

* This applies for siliceous soils. For calcareous soils, we assume $m_s^g > 0$ only if $T_g > 3100^\circ$.

where Λ is given by the height of burst (ft) divided by $W^{1/3.4}$, and $z = -\Lambda$. For $T_g < 3000^\circ$, we found that energy balances are obtained for all pertinent yields. Above 3000° , we computed values of T_c for values of m_s^g obtained from the relation

$$m_s^g = p \left(\frac{T_g - 3000}{100} \right) m_s, \quad (B.13)$$

where m_s is the total soil burden and p , the fraction of the soil burden vaporized per 100° excess of the initial temperature over 3000° , ranged from 0 to 0.017.

The solid curve of Figure B.2 shows unvaporized soil temperatures computed as indicated above. This curve remains substantially the same for any height of burst. For yields greater than about 10^3 KT, vaporized soil is predicted to remain in the cloud at time t_1 . Beyond this yield we have plotted temperature curves for several values of p from Eq. (B.13). According to these curves, temperature of unvaporized soil increases as p increases. This is an artifact of the particular mode of setting up the energy partitioning and is illustrative of the sensitivity of the calculation to even minor variations in such procedures. Since the overall spread of temperature is only 300° and, in addition, the model design is rather arbitrary, we need not be particularly concerned by it.

The dashed curve of Figure B.2 shows the temperature relationship chosen (rather arbitrarily) to provide values of T_c for fallout prediction calculations; it is described by the relation

$$T_c = 50 \log_{10} W + 1400. \quad (B.14)$$

This expression yields satisfactory energy balances except for low yield subsurface bursts. For example, at $W = 10^{-2}$ KT and $\Lambda = -20$, $f = 1.16$. That the method should fail for these conditions is not at all surprising since our gas temperature values for surface bursts are quite suspect at the extreme low end of the yield range and they scarcely apply at all to subsurface bursts.

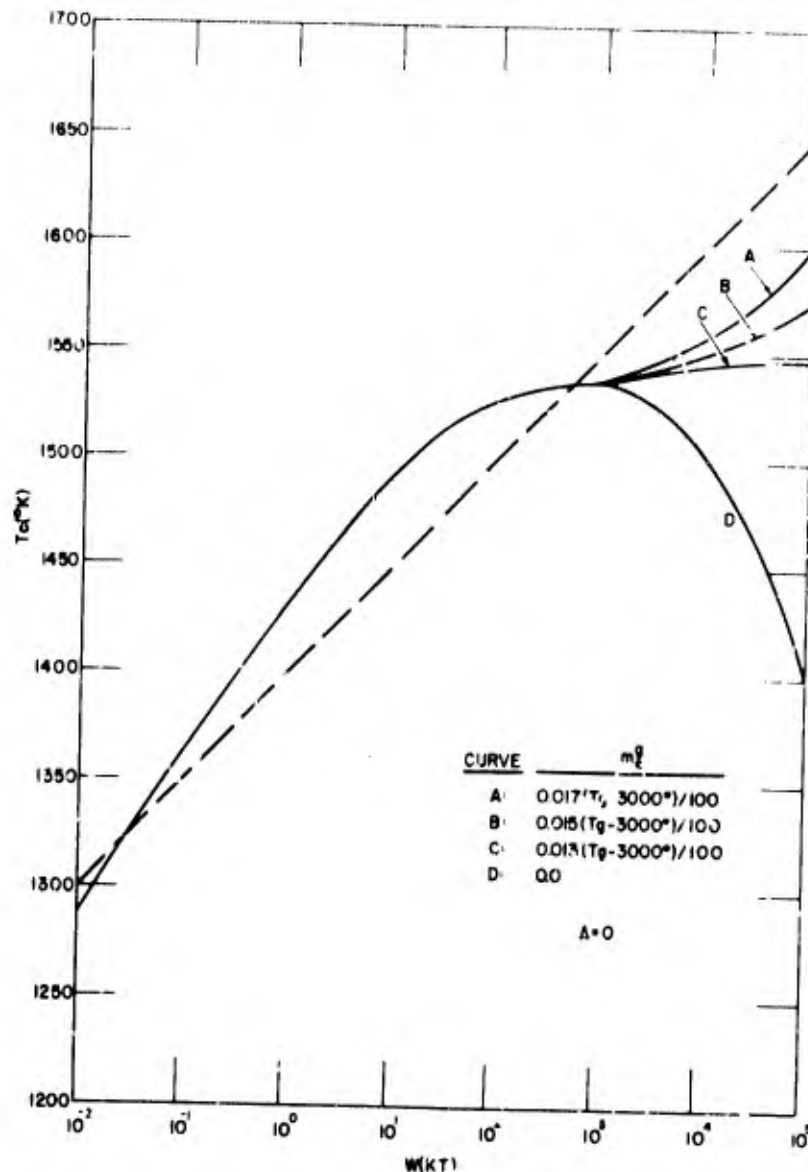


Figure B.2. Computed Temperature of Unvaporized Soil for a Surface Burst

The value of 0.015 for the constant p to be used in fallout prediction calculations (see item 1 on p. 28) was chosen by the following considerations:

1. For p as great as 0.017 at $W = 10^5$ KT, the vaporized soil mass already represents as high as 28% of the total soil burden (at $A = 150$). Thus, there is little incentive to consider a larger p .

2. According to Figure B. 2, the temperature curve begins to level off at yield values less than those for which vaporization occurs. A value for p of around 0.015 seems to provide a reasonable extrapolation of this tendency.
3. 0.015 is a convenient number.

REFERENCES

- B.1 S. Glasstone, editor, "The Effects of Nuclear Weapons, " USAEC (1962, revised 1964).
- B.2 J. Hilsenrath, et al., "Tables of Thermal Properties of Gases, " NBS Circular 564 (1 November 1955), Table 2.3.
- B.3 K.K. Kelly, "Contributions to the Data on Theoretical Metallurgy. XIII. High-Temperature Heat-Content, Heat-Capacity, and Entropy Data for the Elements and Inorganic Compounds, " Bureau of Mines Bulletin 584 (1960).
- B.4 H. L. Schick, "A Thermodynamic Analysis of the High-Temperature Vaporization Properties of Silica, " Chemical Reviews 60, 331 (1960).
- B.5 H. G. Norment and S. Woolf, "Studies of Nuclear Cloud Rise and Growth, " Technical Operations Research, TO-B 66-9 (2 February 1966). Secret-F.R.D.
- B.6 S. L. Valley, editor, "Handbook of Geophysics and Space Environments" (Air Force Cambridge Research Laboratories, 1965; McGraw-Hill Book Company, 1966).
- B.7 "Capabilities of Atomic Weapons, " Dept. of Army Tech. Manual, TM 23-200 (1955). Secret-R.D.
- B.8 J. D. Coughlin, "Contributions to the Data on Theoretical Metallurgy. XII. Heats and Free Energies of Formation of Inorganic Oxides, " Bureau of Mines Bulletin 542 (1954).

Unclassified
Security Classification

DOCUMENT CONTROL DATA - R&D

(Security classification of title, body of abstract and indexing annotation must be entered when the overall report is classified)

1. ORIGINATING ACTIVITY (Corporate author)

Technical Operations Research,
Burlington, Mass.

2a. REPORT SECURITY CLASSIFICATION
Unclassified

2b. GROUP

3. REPORT TITLE

Department of Defense Land Fallout Prediction System
Volume II - Initial Conditions

4. DESCRIPTIVE NOTES (Type of report and inclusive dates)

Final Report

5. AUTHOR(S) (Last name, first name, initial)

H. G. Norment, W. Y. G. Ing, and J. Zuckerman

6. REPORT DATE

30 September 1966

7a. TOTAL NO. OF PAGES

67

7b. NO. OF REFS

44

8a. CONTRACT OR GRANT NO.

DA18-035-AMC-737(A)

a. PROJECT NO.

c. TASK

DASA Subtask A7a/10.058

d.

9a. ORIGINATOR'S REPORT NUMBER(S)

TC-B 66-44

9b. OTHER REPORT NO(S) (Any other numbers that may be assigned this report)

DASA 1800-II

10. AVAILABILITY/LIMITATION NOTICES

Each transmittal of this document outside the agencies of the U. S. Government must have prior approval of the Director, Defense Atomic Support Agency, Washington, D. C. 20301

11. SUPPLEMENTARY NOTES

12. SPONSORING MILITARY ACTIVITY

Defense Atomic Support Agency

13. ABSTRACT

A set of initial conditions to serve as primary inputs to the Department of Defense Land Fallout Prediction System (DELFIC) is derived. The set consists of lower-boundary conditions for use by a cloud rise and growth simulation model. The conditions are time, temperature, soil burden, fraction of the soil burden in the vapor phase, and size-frequency distribution of fallout particles. The DOD Land Fallout Prediction System predicts local fallout patterns from land-surface nuclear detonations.

14.

KEY WORDS

Initial conditions
Fallout
Nuclear weapons effects
DELFAC

LINK A

LINK B

LINK C

ROLE

WT

ROLE

WT

ROLE

WT

INSTRUCTIONS

1. **ORIGINATING ACTIVITY:** Enter the name and address of the contractor, subcontractor, grantee, Department of Defense activity or other organization (corporate author) issuing the report.

2a. **REPORT SECURITY CLASSIFICATION:** Enter the overall security classification of the report. Indicate whether "Restricted Data" is included. Marking is to be in accordance with appropriate security regulations.

2b. **GROUP:** Automatic downgrading is specified in DoD Directive 5200.10 and Armed Forces Industrial Manual. Enter the group number. Also, when applicable, show that optional markings have been used for Group 3 and Group 4 as authorized.

3. **REPORT TITLE:** Enter the complete report title in all capital letters. Titles in all cases should be unclassified. If a meaningful title cannot be selected without classification, show title classification in all capitals in parenthesis immediately following the title.

4. **DESCRIPTIVE NOTES:** If appropriate, enter the type of report, e.g., interim, progress, summary, annual, or final. Give the inclusive dates when a specific reporting period is covered.

5. **AUTHOR(S):** Enter the name(s) of author(s) as shown on or in the report. Enter last name, first name, middle initial. If military, show rank and branch of service. The name of the principal author is an absolute minimum requirement.

6. **REPORT DATE:** Enter the date of the report as day, month, year, or month, year. If more than one date appears on the report, use date of publication.

7a. **TOTAL NUMBER OF PAGES:** The total page count should follow normal pagination procedures, i.e., enter the number of pages containing information.

7b. **NUMBER OF REFERENCES:** Enter the total number of references cited in the report.

8a. **CONTRACT OR GRANT NUMBER:** If appropriate, enter the applicable number of the contract or grant under which the report was written.

8b, 8c, & 8d. **PROJECT NUMBER:** Enter the appropriate military department identification, such as project number, subproject number, system numbers, task number, etc.

9a. **ORIGINATOR'S REPORT NUMBER(S):** Enter the official report number by which the document will be identified and controlled by the originating activity. This number must be unique to this report.

9b. **OTHER REPORT NUMBER(S):** If the report has been assigned any other report numbers (either by the originator or by the sponsor), also enter this number(s).

10. **AVAILABILITY LIMITATION NOTICES:** Enter any limitations on further dissemination of the report, other than those imposed by security classification, using standard statements such as:

(1) "Qualified requesters may obtain copies of this report from DDC."

(2) "Foreign announcement and dissemination of this report by DDC is not authorized."

(3) "U. S. Government agencies may obtain copies of this report directly from DDC. Other qualified DDC users shall request through

(4) "U. S. military agencies may obtain copies of this report directly from DDC. Other qualified users shall request through

(5) "All distribution of this report is controlled. Qualified DDC users shall request through

If the report has been furnished to the Office of Technical Services, Department of Commerce, for sale to the public, indicate this fact and enter the price, if known.

11. **SUPPLEMENTARY NOTES:** Use for additional explanatory notes.

12. **SPONSORING MILITARY ACTIVITY:** Enter the name of the departmental project office or laboratory sponsoring (paying for) the research and development. Include address.

13. **ABSTRACT:** Enter an abstract giving a brief and factual summary of the document indicative of the report, even though it may also appear elsewhere in the body of the technical report. If additional space is required, a continuation sheet shall be attached.

It is highly desirable that the abstract of classified reports be unclassified. Each paragraph of the abstract shall end with an indication of the military security classification of the information in the paragraph, represented as (TS), (S), (C), or (U).

There is no limitation on the length of the abstract. However, the suggested length is from 150 to 225 words.

14. **KEY WORDS:** Key words are technically meaningful terms or short phrases that characterize a report and may be used as index entries for cataloging the report. Key words must be selected so that no security classification is required. Identifiers, such as equipment model designation, trade name, military project code name, geographic location, may be used as key words but will be followed by an indication of technical context. The assignment of links, rules, and weights is optional.